Titre: Title:	Automatic digitization of sculptured parts for NC tool path generation
Auteur: Author:	Yousefali Abbaszadeh-Mir
Date:	1995
Type:	Mémoire ou thèse / Dissertation or Thesis
Référence: Citation:	Abbaszadeh-Mir, Y. (1995). Automatic digitization of sculptured parts for NC tool path generation [Master's thesis, École Polytechnique de Montréal]. PolyPublie. https://publications.polymtl.ca/32690/

URL de PolyPublie: PolyPublie URL:	https://publications.polymtl.ca/32690/
Directeurs de recherche: Advisors:	Marek Balazinski, & J. R. René Mayer
Programme: Program:	Unspecified

UNIVERSITÉ DE MONTRÉAL

AUTOMATIC DIGITIZATION OF SCULPTURED PARTS FOR NC TOOL PATH GENERATION

YOUSEF ABBASZADEH MIR

DÉPARTEMENT DE GÉNIE MÉCANIQUE

ÉCOLE POLYTECHNIQUE DE MONTRÉAL

MÉMOIRE PRÉSENTÉ EN VUE DE L'OBTENTION

DU DIPLÔME DE MAÎTRISE ÈS SCIENCES APPLIQUÉES

(GÉNIE MÉCANIQUE)

JUILLET 1995

REJETEE
A LA BNC

UNIVERSITÉ DE MONTRÉAL

ÉCOLE POLYTECHNIQUE DE MONTRÉAL

Ce mémoire intitulé :

AUTOMATIC DIGITIZATION OF SCULPTURED PARTS FOR NC TOOL PATH GENERATION

présenté par: ABBASZADEH MIR Yousef

en vue de l'obtention du diplôme de: Maîtrise ès Sciences Appliquées

a été dûment accepté par le jury d'examen constitué de :

M. MASCLE Christian, Ph.D., président

M. BALAZINSKI Marek, Ph.D., membre et directeur de recherche

M. MAYER René, Ph.D., membre et codirecteur de recherche

M. DUPINET Éric, Ph.D., membre

À tous ceux qui aiment la science

ACKNOWLEDGMENTS

I would like to thank Dr. Marek Balazinski my supervisor and Dr. Rene Mayer my co-supervisor for their valuable comments, their availability and their support in this work which led to the improvement of this work.

I would also like to thank Mr. Francois Trochu for his availability and for the kind use of his extensive library of Kriging functions.

RÉSUMÉ

Généralement, la fabrication d'un nouveau produit est basée sur une idée transformée en un modèle physique. Le produit est généralement conçu sur la base d'exigences fonctionnelles et esthétiques. Après cela un prototype (en utilisant en matériau comme le bois, l'argile ou le plâtre de moulage) est réalisé et raffiné jusqu'à ce que toutes les spécifications soient rencontrées. Pendant cette première phase, le changement fait sur le modèle original peut être habituellement significatif et complexe. Ces demandes exigent d'utiliser des méthodes d'ingénierie inversée pour régénérer un modèle plus précis.

L'objectif des techniques d'ingénierie inversée est la génération de surface 3-D du produit sous forme de fichier CAO, surtout dans les cas de formes complexes. Pour ce faire, d'abord les coordonnées x, y, z de points multiples sur la surface du produit sont digitalisées. Les surfaces sur modèle CAO peuvent ensuite servir à générer la trajectoire d'outil pour une machine appropriée sous forme d'un fichier contenant le code-G nécessaire.

Ce mémoire propose une procédure de digitalisation de pièces existantes en utilisant une CMM (machine à mesurer à coordonnées). Une CMM est capable de déplacer et de déterminer la position cartésienne du centre d'un palpeur sphérique avec

une précision de quelques micromètres. Le palpeur sphérique est incorporé à l'extrémité de la CMM et amené en contact avec la pièce. Lorsque le contact est établi, les coordonnées du centre de la sphère sont enregistrées. Quand le mesurage des différentes positions est complété, la dimension et la forme de l'objet doivent être évaluées. Étant donné qu'initialement, le centre du palpeur est considéré comme le point de touche, alors une erreur est créée et doit être compensée. Aussi étant donné que les pièces à digitaliser sont souvent inconnues, une autre méthode est proposée pour déterminer le nombre et la position des mesures pour une digitalisation précise et rapide de ces pièces. Pour cela, quelques points sont mesurés initialement manuellement avec la CMM. Ensuite, une surface initiale est générée en utilisant les points initiaux par le modèle de Krigeage. Ce modèle est graduellement amélioré par l'addition de points mesurés en utilisant une méthode adaptative et automatique.

Les travaux futurs devraient être concentrés sur la sélection du palpeur, la planification de l'inspection, la localisation des pièces sur la CMM, la densité d'échantillonnage sur la pièce à mesurer et finalement l'usinage direct de la pièce digitalisée.

ABSTRACT

The task of manufacturing a new product usually begins at the designer's desk where an idea is transformed into a design for a physical model. The product is conceptualized by the designer based on some specified functional and aesthetic requirements. Next, a mock-up (using a soft material such as wood, clay or plaster of Paris) is made and refined till it meets all the specifications. During this process, the changes made to the original model are often so numerous and complex that engineering changes made to the original drawing are typically not accurate enough or are extremely time consuming. This necessitates the application of reverse engineering methods to generate an accurate drawing.

When dealing with complex shapes, the objective of any reverse engineering technique is to generate a 3-D mapping of the product in the form of a CAD file. In order to do this, the x,y,z coordinates of multiple points on the product surface first have to be acquired. These coordinate can then be used to develop the drawing of the product further for redesign or manufacture. CAD/CAM packages that will generate a machining path for the appropriate machines and output a file containing the necessary G-Codes are already available and are being further refined.

This thesis proposes a digitizing procedure for an existing part using a CMM.

A CMM is able to move and determine the cartesian position of the centre of a spherical tip touch probe to accuracies of a few microns. The spherical tip touch probe incorporated in the last body of a CMM is brought in contact with the part. Upon contact the coordinates of the centre of the spherical tip touch probe are recorded. When measurements at various positions are completed, the 3-D size and form of the object must be evaluated. Since initially the probe centre is considered as the touched point, an error is created that must be compensated. Next, since the digitized parts are often unknown, another method is proposed to accurately and rapidly digitize theses parts. For this, initially a number of points are measured under manual CMM operation on the surface. An initial surface is generated using these initial points with a Kriging modeller. The reliability of this initial surface is gradually improved by progressively adding measurement points through an adaptive automatic CMM program.

Future research should be concentrated on the probe selection, inspection planning, part localization on the CMM table, sampling density on the part to be digitized and finally direct machining of the designed part.

CONDENSE EN FRANÇAIS

En matière de technique, où l'ergonomie et l'aérodynamique sont des facteurs importants, le prototype des modèles sculpturé sont souvent faits à le main. Un prototype rapide de tel modèle est nécessaire pour fabriquer le produit en un temps minimum. Idéalement, "digitization" automatique des surfaces, converties les données dans un modèle via l'ordinateur et fabriqué par Fabrication Assisté par Ordinateur(FAO) dans une forme très appropriée. Ce processus est nommé "Reverse Engineering".

Habituellement, la forme de surface dans la majorité des applications(carrosserie d'automobile jusqu'aux l'appareil de ménager) offre une grand nombre de caractéristique distincts, compris les surfaces de "free-form" comme les plans, les cylindres, etc., tout cela pour créer un effet spectaculaire. Actuellement, la "digitization" se fait à travers de mesures faits manuellement ou automatiquement en utilisant une machine à mesure tridimensionnel(MMT).

Les systèmes à vision étant aussi capables de mesurer les points en trois dimensions sur la surface et sont également applicables dans le "reverse engineering". Ces systèmes ont quelques bonnes caractéristiques, lorsqu'ils sont incorporé dans la tâche de "prototype rapide", pour augmenter l'efficacité du processus. Beaucoup de

systèmes à vision emploient une source laser, optique et un détecteur sensible à lumière pour mesurer la distance entre le capteur et la surface. La plupart des techniques basées sur le laser emploie la géométrie triangulaire.

Comparé à un système basé sur la laser, un système de mesure MMT a l'avantage d'être précis, et moins coûtent. L'autre limitation du système à vision est le compromis entre la précision et le champ de vision.

Il y a plusieurs méthodes pour lesquelles peuvent les données peuvent être s'acquisses. Elles peuvent être classés en deux grandes catégories: Les méthodes contact et les méthodes non-contact.

Les méthodes contact furent été utilises pour plusieurs ans. Elles demandent un contact entre la surface de la pièce et l'outil de mesure.

La mesure faite manuellement était la seule technique existant les 30 dernières années pour convertir un modèle physique en dessin. La méthode manuelle est encore en usage dans plusieurs petites usines à travers le monde. Le désavantage de cette méthode est qu'ils exige un nombre d'heures de main d'oeuvre, non seulement pour l'extraction des données mais aussi pour l'entrées des ces données.

La MMT qui permet d'inspecter une pièce en 3-D apparut d'abord au début des ans 1960. Ensuite elles connu un progrès significatif en terme de vitesse et précision des mesures. Une MMT est un appareil de mesure tridimensionnels

qu'utilise un palpeur à contact pour détecter la surface de l'objet. Le palpeur est généralement un appareil sensible à pression qui est déclenché par contact avec la surface. Les distances linaires de déplacement de trois axes sont enregistres et sont représentées en coordonnées x, y, z des points.

La prototype, ou pièce, à mesurer est placé sur la table de mesure de la machine, et les coordonnés des points sur la surface sont acquises. Ces points sont entrés dans un fichier IGES qui peut ensuite être transfères dans un système de CAO pour génère le dessin de la pièce. De cette manière, la figure de l'objet acquise en forme de dessin de CAO, peut être manipulée et modifiée lorsque nécessaire. Après avoir exécuté une surface initiale appropriée où les points sont collectés, la précision du modèle vérifiera, nécessaire, plus de points dans les zones de tolérance et ce d'une façon itérative.

La plupart des méthode non-contact utilisent la lumière pour l'extraction des informations. Les principale techniques disponibles présentement incluent l'usage de système d'éclairage. Ces techniques sont encore dans une étape de gestation. Le méthode non-contact des technologies de "reverse engineering" pour créer un modèle de CAO d'une pièce existante, peut être catégorisées en deux grandes classes. Ces techniques sont expliquées en détail dans ce mémoire.

Ce mémoire expliquera les problèmes majeurs liés à l'utilisation de MMT en

compensation du rayon de palpeur peut s'obtenir en déterminant un vecteur normal sur chaque position mesuré de cette surface initiale. Étant donnés que le procédé de compensation doit considérer les normales ver la surface réelle et non ver la surface du centre du palpeur, les essais ont été conduis pour vérifier que la condition tangentielle de touche était réalisée.

Une autre validation expérimentale en utilisant des surface planes et sphériques avec différents rayons de palpeur était fut aussi concluante pour collaborer la grande précision de cette approche. Une pale de turbine a été mesurée et le résultat montre que la méthode est précise et ce à l'intérieur de domaine de précision et de reproductibilité de la MMT. Par séquence cette méthode devrait aider considérablement aider à la "digitization" de surface "free-form" pour le "reverse Engineering".

Plus de travaux sont nécessaires pour évaluer le nombre minimum et la distribution optimum des points de mesuré pour reproduire fidèlement la surface réel. Aussi la méthode proposée peut constituer la base d'une procédure itérative d'un réseau maillé de points a compensé.

Le deuxième article

Une nouvelle méthode pour la programmation des machines à mesure tridimensionnelle pour les pièces sculpturées et inconnues a été développé. Plusieurs

points sur la surface réelle sont initialement mesurées, sous une forme manuelle de la MMT. Une première surface est générée en utilisant de points initiaux avec un manipulateur de krigeage. La précision de cette surface initial est graduellement augmentée en ajoutant progressivement des points à mesurés. Les nouveaux points ciblés ,pour conduite la MMT, sont choisis en se basant sur la complexité locale de l'estimation courante de la pièce. Les résultats expérimentaux indiquent que la méthode développée est capable de créer un programme pour fournir un modèle précis dans un tolérancement géométrique donné en un tempes minimum.

Dans cette étude, une nouvelle approche sera proposée pour une "digitization" rapide et automatique d'une surface inconnue et complexe en utilisant des données obtenues par une MMT équipée d'un palpeur sphérique. Une surface initiale étant générée à partir de quelques points que sont mesurés manuellement. Après qu'une séries de points cibles sont obtenus, ils deviennent candidats pour le re-mesurage de surface avec une plus grande précision. La procédure de mesurage peut continuer jusque ce que la différence entre les points mesurés et le modèle devient plus petite que la tolérance exigée. Le processus de "digitization" et sa planification sont exécutés automatiquement.

Les avantages de l'approche de la "digitization" par la MMT avec un palpeur sphérique sont:

1) La programmation rapide et automatique pour digitalisation des surface

complexes.

2) La possibilité pour digitalisation des surface inconnu.

3) La temps de mesurage peut être réduite d'une façon significative.

4) La précision du modèle peut augmenter à l'occasion.

TABLE OF CONTENTS

DEDICATION.....iv

ACKNOWLEDGMENTS.....v

RÉSUMÉ.....vi

ABSTRACT.....viii

CONDENSE EN FRANÇAIS.....x

TABLE OF CONTENTS.....xvi

LIST OF TABLES.....xx

LIST OF FIGURES.....xxi

CHAPTER 1: INTRODUCTION: Reverse Engineering

1.1 Introduction.....2

1.2 Surface Measurement Techniques.....3

1.2.1 Contact method.....3

1.2.1.1 Manual measurement.....4

1.2.1.2 Coordinate measuring machines(CMMs).....5

1.2.1.3 Electromagnetic digitizing.....6

1.2.1.4 Sonic digitizing.....7

1.2.2 Non-contact method.....7

1.1.2.1 Structured lighting.....8

1.2.2.2 Spot ranging.....10

1.3 Surface description.....12

1.4 CNC machining of reconstructed surface.....14

1.4.1 Tool-path generation for free form surface.....16

1.5 The Proposed solution.....17

CHAPTER 2: (paper 1)

TOUCH PROBE RADIUS COMPENSATION

FOR COORDINATE MEASUREMENT USING

KRIGING INTERPOLATION.....20

Abstract.....21

2.1 Introduction.....22

2.2 Surface Description 24

2.2.1 Parametric curve.....26

2.2.2 Parametric surface.....28

2.2.3 Surface normal vector.....32

2.3 Compensation procedure.....32

2.3.1 Measurement and generation of probe centre surface.....33

2.3.2 The compensated surface.....34

2.4 Experimental Results.....34

2.4.1 Test with reference artefact.....35

2.4.2 Test with a free-form surface.....36

2.5 Discussion and conclusion.....38

References.....40

CHAPTER 3: (Paper 2)

ADAPTIVE MEASUREMENT STRATEGY OF

UNKNOWN SCULPTURED SURFACES ON A

COORDINATE MEASURING MACHINE.....48

Abstract.....49

3.1 Introduction.....50

3.2 Surface Generation.....52

3.2.1 Parametric surface.....53

3.2.2 Surface normal vector.....57

3.3 Proposed adaptive measurement strategy.....58

3.3.1 Generation of an initial surface using manually measured point.....59

3.3.2 Calculation of the target points.....60

3.3.2.1 Generation of the target point.....61

3.3.3 Measuring the part using the target points.....63

3.3.4 Comparison of the measured and the target points.....64

3.4 Validation.....64

3.5 Conclusion and Future work.....66

Acknowledgements.....67

References.....68

CHAPTER 4:

CONCLUSIONS AND RECOMMENDATIONS.....77

References.....80

LIST OF TABLES

Table 2.1 RMS value of the distance between the measured and predicted probe centre points calculated from the compensated surface.....42

Table 3.1 Geometry information of the generated surface of each procedure...70

Table 3.2 The results of procedure evaluation.....70

LIST OF FIGURES

Figure 2.1 The tangential condition between the touch probe and the part.....42

Figure 2.2 2D curves used to generate a 3D surface.....43

Figure 2.3 Sculptured surface generated using kriging.....43

Figure 2.4 Probe centre surface with its normal vectors.....44

Figure 2.5 The compensation of the probe centre points using the probe centre surface normals.....44

Figure 2.6 Original and offset surface.....45

Figure 2.7 Compensated surface generated for a flat part.....45

Figure 2.8 Compensated surface generated for a hemisphere.....46

Figure 2.9 The relationship between the measured probe centre ($P_{p,i}$), the compensated point ($P_{c,i}$) and predicted probe centre point ($P_{p,i}^{*}$) based on the tangential condition of the touch.....46

Figure 2.10 Turbine blade used for evaluating the method.....47

Figure 2.11 Compensated surface generated for a turbine blade.....47

Figure 3.1 Measurement errors resulting from an incorrect surface normal vector.....71

Figure 3.2 A sculptured surface generated using the kriging method.....71

Figure 3.3 The target points and normal directions.....72

Figure 3.4 The schematic diagram for the procedure of the adaptive measurement method.....72

Figure 3.5 The target point and the corresponding measured point.....73

Figure 3.6 Approximating curvature: (a) osculating circle (b) ratio of tangent angle to arc length.....73

Figure 3.7 A schematic diagram for procedure calculation of target point.....74

Figure 3.8 The values of Δm for different curves.....74

Figure 3.9 Relationship between Δm_c and $\Delta \theta_{max}$ 75

Figure 3.10 Relationship between the target points, normal vectors and measured points.....75

Figure 3.11 Target point location for the initial and subsequent iteration.....76

Figure 3.12 The final generated surface from the digitized part.....76

Chapter 1

Introduction: Reverse Engineering

1.1 INTRODUCTION

In engineering design, where style, ergonomic and aerodynamic factors are important, clay prototype of sculptured models are often created by hand in design studios [1]. Rapid prototyping of such models is then needed in order to manufacture the product in minimum time. Ideally, this entails automatic surface digitization, conversion of data to computer based models and computer-numerically-controlled (CNC) manufacture in the most appropriate form. This process is called "reverse engineering". The surface shape in the majority of applications (from automobile body panels through to household appliances) usually contains many separate and distinct features, including free-form surface patches as well as planes, cylinders, etc, all blending together to create a stylish effect. Currently, the digitization is done through measurements taken manually and automatically using a coordinate measuring machine (CMM).

Computer vision system are also capable of measuring three-dimensional points on a surface, and can be applied to reverse engineering. They have some beneficial features that, when incorporated into rapid prototyping tasks, can increase the efficiency of the process. Most vision systems employ a laser source, optics and a light sensitive detector to measure the distance between the sensor and the surface. The most common laser technique employs the triangular geometry formed by the locations of the laser source, diffusely reflected laser beam, focusing lens and imaged laser spot on the light sensitive detector. Compared to a laser-based system, CMM surface measurement has

the advantage of being more accurate. CMMs are also more commonly found in industry.

In rapid phototyping applications, the data generated by a CMM will be incorporated into a CAD system. Direct CNC machining of the scanned data is not possible because the set of digitized surface points do not necessarily define a suitable path for the cutting tool to follow. Also if the surface data generated is not smooth or makes sudden jumps in height between regions on a surface, then the cutter path will be erratic and unsuitable.

In this thesis an investigation into new approaches for using CMM for the digitization of parts is presented. Methods for modelling digitized curves and surfaces are also described. An approach to compensate errors, due to the probe radius by an offset surface method using kriging is given. Finally a measurement planning approach for digitizing unknown curves and surfaces is proposed.

1.2 SURFACE MEASUREMENT TECHNIQUES

There are several methods by which product profile data can be acquired. They can be classified into two broad categories: Contact and non-contact methods.

1.2.1 Contact Methods

Contact methods for generating the part profile have been in use for several years.

All these methods require a contact between the component surface and a measuring tool which is usually a probe or stylus.

1.2.1.1 Manual measurement

This was the only existing technique until about 30 years ago to convert a physical model to a drawing. This method is still in use in several small factories across the world. Here, the evolution of a CAD drawing comprises the following steps : 1) Several key points across the surface of a product are identified and the x, y, z, coordinates are manually measured from a fixed reference point; 2) These points are entered into a CAD system; 3) The curves and surfaces that interpolate these points are then generated. In this way, a 3-D CAD model of the product is created. Instruments that are commonly used include callipers, measuring gages and blocks. The number of points across the part surface ranges from less than 10 for a simple symmetric part to over 2000 points for more complex surfaces.

The disadvantage of this method is the number of man-hours it requires, not only for the data extraction, but also for data entry. Also, the accuracy of the method depends on the precision and accuracy of the callipers and other measuring instruments. Another reason for the reduced accuracy is that fewer points than required are usually measured due to the effort involved.

1.2.1.2 Coordinate Measuring Machines (CMMs)

CMMs that could inspect a 3-D part first appeared in the early 1960s. Since then, they have advanced significantly in terms of speed and accuracy of measurement, and the available peripheral equipments. They have now become an integral part of the inspection system of many companies. Due to their widespread use, CMMs are the most popular tool used to implement reverse engineering techniques.

A CMM is a three-dimensional measuring device that uses a contact probe to detect the surface of the object. The probe is generally a sensitive pressure-sensing device that is triggered by any contact with a surface. The linear distances moved along the three axes are recorded, thus providing the x, y, z coordinates of the point. CMMs are classified as either vertical or horizontal according to the orientation of the last joint with respect to the measuring table.

Coordinate measuring machines can further be classified according to their geometry such as table cantilever, moving bridge, fixed bridge, column, moving ram horizontal arm, moving table cantilever arm and gantry. A typical medium size, moving bridge type machine manufactured by LK Tool Ltd. model G90c 8.7.6 was used in this work.

The prototype, or part, to be measured is placed on the measuring table, and the coordinates of a number of points on the surface of the object are taken. These points

are entered into an IGES file that can then be transferred to a CAD system to generate the drawing of the part. In this way, the shape of the object is captured in the form of a CAD drawing that can be manipulated and modified as needed. After performing an initial surface fitting to the collected points, the accuracy of this model is verified. If necessary, more points, from the "out of tolerance" areas, can be collected to iteratively perfect the model.

1.2.1.3 Electromagnetic digitizing

The use of electromagnetic transducers to digitize 3-D objects is a recent development [2]. The product to be digitized is placed on a model table. This table encloses the electronic equipment and a magnetic field source which creates a magnetic field in the volume of space above the table. A hand-held stylus is used to trace the surface of the part. This stylus houses a magnetic field sensor which, in conjunction with the electronics unit, detects the position and orientation of the stylus. The data is then transmitted to a host personal computer via an RS-232C serial port. The system has the capability to transmit either individual data points, or to send a stream of points which are detected by continuous sampling at the rate of 60 points per second. Therefore complex curved surfaces can also be digitized.

The main advantage of this system is that it costs less than a CMM while still being sufficient to meet reverse engineering needs. However only non-metallic objects can be measured using this technology. Also, making corrections to the model by

collecting additional data points is not easy. Therefore, iterative improvement of the model is not facilitated.

1.2.1.4 Sonic digitizing

A sonic digitizer uses sound waves to calculate the position of a point relative to a reference point [3]. In this approach, the object is placed in front of a vertical rectangular board on the corners of which are mounted four microphone sensors. A free, hand-held stylus is used to trace the contours of the object. When a foot or hand switch is pressed, the stylus emits an ultrasonic impulse and simultaneously four clocks are activated. When the impulse is detected by each of the four microphones, the associated check count is recorded. These time recordings, called slant ranges, are processed by the host computer to calculated the X, Y and Z coordinates of the point.

Some of the advantages of this method are: it has a larger active volume than the electromagnetic method, any substance (including ferrous materials) can be digitized. It is reasonably insensitive to the background noise; therefore it can be used in less controlled environments. A disadvantage is that it is difficult to get a set of points on a continuous basis; therefore contour tracking is more difficult.

1.2.2 Non-contact method

Non-contact methods use light as the main tool in extracting the required information. The main techniques which are presently available include the use of

structured lighting. These techniques are still in an evolutionary stage. The non-contact reverse engineering technologies for creating a CAD model of an existing part can be classified into two broad classes: active and passive. Active methods require the use of a technique that can be further divided into two main categories: structured lighting and spot ranging. These technologies are described below.

1.2.2.1 Structured lighting

This method can be further classified based on the pattern of light that is used to illuminate the part. The various light patterns that are used include a single light beam, a single stripe of light, multiple stripes of light, or patterned lighting such as grid-coded illumination and moire topography.

The general methodology here, is to reflect a single laser beam off the part and detect the position of the deffused beam using a sensor, such as a camera. The part's image on the camera reveals the 2-D coordinate of the surface point. Since this point is located at the intersection of the line of the light source and the line of the camera axis, triangulation procedures are used to calculate the depth of the point [4]. In this way, the entire part surface can be digitized by sweeping the light source over the surface. This is sometimes achieved by using a computer controlled rotating mirror system [5].

The speed of data acquisition can be increased by collecting information about an array of points on the surface. This is done by spreading the laser beam, using a

cylindrical lens, into a vertical light stripe. Triangulation can then be used to find the depth information for several points on the stripes.

One of the earliest systems using this method consisted of a slit projector that was mounted on a rotary table, a TV camera and a computer [6]. The boeing Company developed a system to manufacture tiles for the space shuttle. The sides and bottom of the tile cavity were scanned to retrieve the geometry information, which was used by an NC post processor to generate the NC part program [7]. A recent system also incorporates a CAD interface to generate the CAD drawing of the part automatically [4].

To further speed up the data collection process, multiple stripes of light can be reflected off the surface of the part. This is one of the methods that is being studied for the real-time data acquisition for robot vision. One of the problem with this method is the difficulty in determinting the correspondence between the incident light stipes and their reflected images. The high processing requirements may thus offset the advantage of increased speed.

Another approach to structured lighting is to illuminate the workpiece surface with different light patterns. The grid coded illumination and moire topography techniques belong to this category.

In grid coded illumination, different masks are used to create various patterns of

light. The part is successively illuminated with the different light patterns, and surface information is retrieved from the resulting images. The advantage of this method is that the entire surface is not scanned, as in previous methods, thus reducing the processing time. The accuracy of this method depends on the width of the light bands that comprise the patterns, the thinner the bands, the greater the accuracy.

Moire topography involves the illumination of the surface with patterns of light that are obtained by passing the light through an optical grating. When the surface is viewed through an identical grating, the resulting fringe patterns are analyzed to retrieve the contour information. Analysis can be done by comparing the fringe pattern with that for a plane surface, and finding the deviations using a digitizing method. The grating period can be adjusted to increase the sensitivity of this method.

1.2.2.2 Spot ranging

There are two broad classes of spot ranging methods, based on the source used. These are optical based methods and ultrasonic methods. Both methods involve the projection of a beam onto the object surface, and inspection of the reflected beam using a sensor that is placed coaxial to the source. The location of the source gives the x, y coordinates of the surface point, while analysis of the reflected beam gives the range of the point.

In optical methods, the reflected beam can be analyzed in two different ways.

The first method is used to calculate the phase difference between the incident and reflected light, thus revealing the range of the surface being recorded. Accuracies are generally higher for the phase difference technique due to limitation on the sensitivity of the timing devices. The entire surface of the part is raster scanned to generate the complete 3D image. An advantage of this method is that the coaxiality of the source and receiver eliminates the problem of missing points. However, almost all optical system are relatively expensive.

Ultrasound methods involve the generation of ultrasound pulses that are reflected off the surface of the part, and detected by a sensor. The time of flight is used to find the range of the surface point. The accuracies of these system are typically less than those for the optical systems since it is difficult to generate narrow beams of sound.

The passive non-contact techniques comprise three different methods: range from texture, range from focus and stereo scanning.

Range from texture: The principle of this technique is the known fact that the further one goes away from an object, the smoother its surface texture appears to be. Therefore, if the texture of an object is known, its distance from the viewpoint can be estimated by inspecting the perceived texture. However, limitation in accuracy have precluded its use thus far in reverse engineering.

Range from focus: This technique uses the fact that when an object is viewed though a lens, the distance of the resulting image from the lens is dependent on the focal length of the lens and the distance of the object from the lens. This can be used to find the range of the points on the surface of a part. However, these system have not been used for reverse engineering due to their limited accuracy.

Stereo scanning: Here, two images of the object are captured by viewing from two different viewpoints. Then, the corresponding surface points on the two images are identified. A triangulation procedure is then used to find the range of the point. The difficulty of this method lies in the identification of the matching image pixels that correspond to the same point on the object. Most available algorithms are computationally intensive and time-consuming [7].

1.3 SURFACE DESCRIPTION

The design of free-form objects with CAD often involves the use of physical models at some stage of the design process. The initial aesthetic design of products having sculptured surfaces (e.g., consumer electronics, household equipments, car and aircraft bodies, etc.) is still often done by industrial designers who formalize their ideas by producing a wooden or clay model. The geometry of the hand-made model must often be introduced in a CAD system for further design or manufacturing. Physical models are also often used even if a CAD design already exists. Typical examples can be found in the aeronautical and automotive industry, where physical models are also

produced at the later design stages for wind-tunnel tests. Such tests generally result in manual modifications and optimization of the physical model. The original CAD model must then be modified based on the new shape of the modified physical object. In the mould and die making industry hand-made models are often the only available source of information on the product. They are also often the preferred source of information on the product and are used as means of communicating between contractors. In such cases, people often need to introduce the geometry of the hand-made models into CAD.

Similar problems may also occur at the product inspection stage. After a product has been produced, its free-form shape has to be measured and reentered into a CAD system for comparison with the toleranced geometry.

Free-form shape reconstruction in a CAD system is mostly based on digitized data obtained with a coordinate measuring machine (CMM). The most popular CAD/CAM systems generate a free-form surface through a grid of digitized points. This can sometimes cause problems if the grid points are not property selected, if there are not enough or too many digitized points or if random errors are included in the digitized data. Random errors generally result from the limited accuracy of the coordinate measuring machine and introduce instabilities in the interpolated surface. When this is the case the interpolated surface will often deviate far from the true surface in between the digitized points. Specialized free-form digitizing software are mostly based on Bézier interpolation algorithms. Since Bézier algorithms are suited to model only small surface

patches, the surface must often be divided into many segments and discontinuity problems may occur across the borders of adjacent patches. Non-uniform rational B-splines (NURBS) surface are used to represent the identified free-form shape. With NURBS surfaces it is possible to handle, large surface patches, to deal with discontinuities and to have better local control and smoothness control [8]. In this thesis an alternative algorithm for CAD modelling using digitized data taken with coordinate measuring machines is presented. A Kriged surface is used to define the digitized surface with a set of digitized points. The method used to reconstruct the curve and surface using this method will be explain latter. The key reason for using this algorithm was that the Kriging library of functions, developed in École Polytechnique de Montréal, was readily available and its applicability in this context was not known. But appeared promising[9, 10].

1.4 CNC MACHINING OF THE RECONSTRUCTED SURFACE

For machining surface patches, a milling cutter suitably positioned relative to the surface vertices is directed from vertex-to-vertex across the surface mesh with linearly interpolated motion. The steps to achieve this are outlined below and are also given in Vickers, Ly and Oetter [11].

1. The selection of a surface resolution suitable for complete surface machining. The determination of the number of surface vertices at which machining occurs is a compromise between the surface roughness and the machining time. Surface roughness

is measured by the size of the cusps left on the surface by the cutting tool.

2. Calculation of the surface vector normal at each surface vertex in order to correctly position the cutting tool relative to the surface form.

3. Calculation of the cutter location by determination of the tool offset, in the direction of the surface vector normal, by an amount dependent on the selected cutter's radii and shape.

4. Generation of a part program in CNC machine code (G-code) that contains additional machining information, such as feedrate and spindle speed.

Techniques for generating the surface vector normal and cutter offset location are developed [11, 12]. Specifically, vector normal calculation for free-form surface patches modelled using kriging interpolation are outlined in chapter 2. Before proceeding with the discussion, it is necessary, however, to first differentiate between the two principal modes of tool movement possible in a CNC machining centre. A linear interpolation command moves the cutter from the current location to a specified location at a given feedrate along a straight line. The CNC machine linear interpolation command format is:

G01 X <*x new* > Y < *y new*> Z <*z new*> F <*federate*>

A circular interpolation command moves the cutter from the current location to a specified location at a given feedrate along a circular arc; the format of the command is:

G02

} X <*x new* > Y < *y new*> R <*radius of arc*> F <*federate*>

G03

A G02 command results in clockwise motion and a G03 in counter-clockwise motion. Circular interpolation movements are specified in one plane (G17, G18, G19) prior to the command being executed.

1.4.1 Tool-path Generation for Free form Surface

In curved surface machining, the cutting tool moves between individual surface vertices in a linear point-to-point manner. Assuming the surface is well defined at a suitable resolution, the surface normal vector n must be calculated for each surface vertex. The vector normal is found directly from the surface modelling function [12].

$$\vec{n}\,(x_0,\ y_0) = \nabla S(x_0,\ y_0) \tag{1}$$

Here, $S(x_0, y_0)$ is given by

$$S(x_0\ ,\ \ y_0) = \sum c_i\ [(x_0 - x_i)^2 + (y_0 - y_i)^2 + b^2]^{\frac{1}{2}} \tag{2}$$

Once the normal vectors are calculated, the reference location on any cutting tool must be offset an appropriate distance in order that the tool cutting point touches the surface at the correct location. The method used for calculating the offset depends on the tool type (ball-mill, end-mill, or generalized shaped end-mill).

The final step is to form the CNC machine code file that is downloaded to a CNC machine centre in order to control the machining process. The G-code file is a standard command set that governs the motion of the cutter from point-to-point in short, straight

line, linearly interpolated motions, Additional information imparted to the G-code file before downloading is:

- The start location (X Start, Y Start, Z Start) at which the cutter is positioned at the beginning of the program.
- The feedrate (units/minute) at which the cutter travels when moving between machining vertices.
- The spindle speed of the cutting tool in revolution per minute.
- The measurement system in inches or millimetres.
- The safety height at which the cutter will travel to get to new machining locations.

The G-code file is then downloaded over a RS 232 serial link to the CNC controller.

1.5 THE PROPOSED SOLUTION

In recent years CMMs have become more and more popular because of their precision and numerical control. They have been used first for quality control applications and today their role in reverse engineering applications is recognized. We used the CMM to digitize complex shape objects.

The steps for digitizing the object are as follows :

1- Open a data file for the new object on the system.

2- Place the object to be digitized on the table of the machine and define its reference

frame.

3- Select the radius of the probe, unit of measurement, velocity, feed and speed of the machine.

4- Select the location of the points if it is the first part.

5- Digitize the object using either a manual or automatic method.

6- Reduce the number of digitized points if necessary.

8- Generate the final CAD model.

The digitizing procedure is the first of three steps (digitizing, modelling and machining) in reverse engineering. This thesis addresses the digitizing and modelling of an object for the generation of NC code.

During the digitization of the object by CMM, the machine initially records the coordinate of the centre of ruby when it touches the object. So, an error is produced that must be compensated. The proposed solution uses the probe centre points to generate an initial estimate of the surface. This probe centre surface is then used to calculate the local surface normals for the compensation of the measured points.

The other problem is the optimisation of the selection of the number and location of the measured points to provide an accurate and efficient digitization procedure. The proposed solution uses an initial set of manually selected measured points to control in an automatic fashion, the taking of subsequent measurements. A criteria is used to assess

the local complexity of the surface in order to decide on the number of points to be added. The procedure automatically stops when the desired accuracy has been reached.

Chapter 2

Paper 1

"Touch Probe Radius Compensation For Coordinate Measurement Using Kriging Interpolation"

Paper written by R. Mayer, Y. A. Mir, F. Trochu , A. Vafaeesefat, M. Balazinski and submitted to the *Proceeding of the Institution of Mechanical Engineering, Journal of Engineering Manufacture.*

Abstract

Obtaining CAD descriptions of actual parts having complex surfaces, is a key part of the process of reverse engineering. This paper is concerned with the estimation of actual surfaces using coordinate measuring machines fitted with a spherically-tipped touch probes. In particular it addresses in detail the problem of probe radius compensation. A general mathematical model, using kriging, is proposed which first generates the initial probe centre surface and then estimates the compensated or part surface. The compensation is achieved using normal vectors to the initial probe centre surface at each measured point to compensate for the probe radius. The method is validated experimentally on known and free-form surfaces.

Keywords: Coordinate measuring machine, probe compensation, surface digitization, compensated surface, reverse engineering.

2.1 INTRODUCTION

The determination of an estimate surface from a physical engineering part with complex surfaces is required in many manufacturing sectors, such as turbine blade manufacture, car model development and surface milling (1). The estimated surface can then be used to generate a large number of surface points and normals for the programming of NC tool paths. The estimated surface is also used in reverse engineering applications. Currently, mechanical coordinate measuring machines (CMMs) are widely used in these areas as the preferred method of digitizing the part geometry.

The CMM uses a sensor to interface with the part to be measured. Currently the most common sensors are either the touch trigger probe or optical sensors such as a laser sensor or a laser point depth probe. Bradley et al. (2) have used a laser scanner for acquiring large quantities of surface points in a relatively short time. This insure that the information about the surface shape is complete. It also allows the use of fitting algorithms to average out the uncertainties in the measurements which in this case are of the order of ± 0.1 mm. In any case, data reduction is usually required, if only to provide a more manageable computer model. Also access to the part may be limited by the physical size and optical constraints of the sensor. Finally scanners add considerably to the total system cost. However the main limitation with touch probes is the time required for digitizing. This is partially offset by the fact that fewer points are needed since a high precision is obtained and no fitting through a large number of points needs to be done.

One of the requirements to ensure the generation of an accurate compensated surface from digitization is the determination of the coordinates of the point where the probe contacts the object to be measured. Two methods for determining the probe contact point have been developed. The first method is based on a new touch probe which can directly detect the contact point. Aoyama and Kawa (3) developed such a touch probe based on a spherical potentiometer. This hardware method requires complex and accurate mechanisms and it remains very difficult to manufacture small probes with fine discrimination at a reasonable cost.

The second method finds the normal direction at the measurement point so that the probe can approach this point along this direction. In this method, CAD data are used to generate the CMM measurement paths (4) (5) (6) (7). However in many prototype development applications, the CAD data may not be available and it is necessary to perform the digitization of mathematically unknown free-form curves or surfaces.

This paper deals with the surface digitization using CMMs and the compensation of a spherical touch probe radius to generate the compensated surface from the probe centre positions.

A CMM provides the Cartesian position of the centre of its spherical tip touch probe to accuracies of a few microns. The CMM probe is brought in contact with the part and upon contact the coordinates of the centre of the probe are recorded. When

contacts at various positions are completed, the 3-D size and form of the object must be evaluated. Since initially the probe centre is considered as the touched point an error is created that must be compensated. As illustrated in Figure 2.1, since the probe and part surfaces are tangential at the contact point, the probe centre point $P_{p,i}$ is offset by one radius R from the touched point on the actual surface of the part $P_{a,i}$ in the direction of the normal vector $N_{a,i}$ to the object surface. Thus at the touched points, it is necessary to generate a good estimate of the normal vectors $N_{a,i}$. Kriging interpolation is used to represent the complex surface and to generate the normal vectors at the measured points.

Section 2 of this paper describes how a complex surface can be represented using kriging interpolation. The method for compensating the probe radius is proposed in section 3. Finally in section 4, experimental results are presented and discussed, followed by a conclusion.

2.2 SURFACE DESCRIPTION

In this section, we consider modelling the surface by interpolating a suitable mathematical model directly to the measured data. Among the great number of surface description techniques available, note that Coons and Ferguson surfaces (**8**) are built up from an array of four-sided surface patches. The Coons surface patch is defined by four boundary curves, whereas the Ferguson surface patch is defined by a position vector, two tangent vectors, and a twist vector at each of the four patch corners. Bézier surface and B-spline surfaces (**8**) are defined by an array of position vectors or a characteristic

polyhedron. Surface kriging is a new method to represent sculptured surfaces. It was first proposed by Gilbert et al (**9**). It is presented in a more general framework by Trochu et al (**14**), who applied the method to model various types of surfaces. It presents two main advantages: (1) *its accuracy*, because the surface is represented by a continuous and differentiable parametric expression; (2) *its generality*, because piecewise linear surfaces, "B-spline" and Bézier surfaces are particular cases of kriging and least square methods can be derived as a limit case (see (**13**)). Another useful characteristic of kriging as is the case of any continually differentiable mathematical model, concerns the determination of the normal vectors at any point of the surface, which can be computed exactly from the kriged mathematical equation of the surface. A formal description of parametric surface kriging now follows.

Kriging is a statistical technique proposed in 1951 by Krige (**10**) for natural resource evaluations. Later, Matheron (**11**) established the mathematical foundation of the method. As presented in the mathematical framework of geostatistics, kriging is simply the best linear unbiased estimator of a random function. The equivalent dual kriging formulation was later proposed by Matheron (**12**). A complete derivation of the basic kriging equations and the connection with dual kriging can be found in Trochu (**13**).

If a deformable curve $\mathbf{P} = \mathbf{P}(s)$ moves in a three dimensional space (see Figure 2.2), the successive positions of the curve generate a surface, each point of which being

identified by its parameters on the moving curve at a given time t. Thus a parametric equation of the form $\boldsymbol{P} = \boldsymbol{P}(s,t)$(see Figure 2.3) describes a three-dimensional surface, with component functions $x = x(s,t)$, $y = y(s,t)$, $z = z(s,t)$. A parametric surface is defined by two kriging profiles along the s and t directions. A kriging profile consists of two parts, a drift and a generalized covariance, which govern the shape of the parametric surface. The drift represents the average shape of the surface, whereas the generalized covariance generates a set of fluctuating terms which enable the data points to be interpolated. Each profile generates a set of curves that move in space.

2.2.1 Parametric curve

The mathematical expression for the x-, y- and z- coordinates of a point P of the surface are functions x(s,t), y(s,t) and z(s,t). A general position vector $P(s, t)$ on a patch is denoted by

$$P(s,t) = [\ x(s,t) \quad y(s,t) \quad z(s,t)\ ]^T . \tag{1}$$

In the three-dimensional space of Cartesian coordinates x, y and z, the parametric equation of a curve is defined by three functions $P(t) = \{x(t), y(t)\ z(t)\}$. Dual kriging permits to construct automatically the equations of smooth parametric curves from a discrete number of measured points $P_i(x_i, y_i, z_i)$. For example, in the case of a linear drift and cubic covariance, the parametric equation of a kriged curve interpolating N data points can be written as follows:

$$P(t) = a_0 + a_1 t + \sum_{j=1}^{N} b_j |t - t_j|^3 . \tag{2}$$

where a_0, a_1, a_2 are the vectors and the parameters t_j , $1 \leq j \leq N$, denote an approximation of the curve length calculated from $t_0 = 0$ by

$$t_{i+1} = t_i + [(x_{i+1}-x_i)^2+(y_{i+1}-y_i)^2+(z_{i+1}-z_i)^2]^{\frac{1}{2}}, \quad 1 \leq i \leq N-1 \ . \tag{3}$$

The first two terms of formula (2) represent the average shape of the curve in the form of a linear drift; the cubic functions in the summation are corrections to the average shape and are given by a cubic shape function $K(h)=h^3$, with $h=|t-t_j|$. In kriging, the average shape may be represented by any kind of polynomial or trigonometric function. The fluctuations of the second set of terms are usually derived from a shape function $K(h)$ called *generalized covariance*. The most widely used generalized covariances in kriging are the cubic, $K(h) = h^3$, logarithmic, $K(h) = h^2 \ln(h)$, and linear, $K(h) = h$. It can be shown that, together with a linear drift, these generalized covariances generate a kriging system that is equivalent respectively to 1D, 2D and 3D spline interpolation (see Matheron (11)).

The coefficients a_0 , a_1 and b_j are obtained by requiring first that the interpolation model (2) fits the data points

$$P(t_i) = P_i(x_i,y_i,z_i), \quad 1 \leq i \leq N \ . \tag{4}$$

Since there are N+2 unknowns, two additional equations must be added to the above N equations. They are obtained by adding the no-bias conditions for a linear drift (see ref. **(13) (14)**):

$$\sum_{j=1}^{N} b_j = 0, \qquad \sum_{j=1}^{N} b_j\, t_j = 0\ . \tag{5}$$

The above expressions are called no-bias conditions because, in the theory of kriging, this implies that the average behaviour of the phenomenon follows a linear pattern (see ref. (11) (13)).

Equations (4) and (5) are sufficient to determine the coefficients a_0 , a_1 and b_j of the parametric model. They can be summarised by a linear system of simultaneous equations written in matrix notation as follows:

$$\left[\begin{array}{ccccc|cc} \cdots & \cdots & \cdots & \cdots & \cdots & 1 & t_1 \\ \vdots & \cdots & \cdots & \cdots & \vdots & \vdots & \vdots \\ \vdots & \cdots & |t_i-t_j|^3 & \cdots & \vdots & 1 & t_i \\ \vdots & \cdots & \cdots & \cdots & \vdots & \vdots & \vdots \\ \vdots & \cdots & \cdots & \cdots & \vdots & 1 & t_N \\ \hline 1 & \cdots & 1 & \cdots & 1 & 0 & 0 \\ t_1 & \cdots & t_j & \cdots & t_N & 0 & 0 \end{array}\right] \cdot \begin{bmatrix} b_1 \\ \vdots \\ b_i \\ \vdots \\ b_N \\ - \\ a_0 \\ a_1 \end{bmatrix} = \begin{bmatrix} P_1 \\ \vdots \\ P_i \\ \vdots \\ P_N \\ - \\ 0 \\ 0 \end{bmatrix} \tag{6}$$

2.2.2 Parametric surface

A three-dimensional surface is described by a parametric equation of the form $\boldsymbol{P} = \boldsymbol{P}(s,t)$, with component functions $x = x(s,t)$, $y = y(s,t)$, $z = z(s,t)$. A parametric surface is defined by two kriging profiles A and B along the s and t directions respectively. The parametric equations of a curve in the s direction (with parameter t constant) for a kriging profile with a linear drift and a generalized covariance $K_a(h)$ can be written as follows :

$$P_t(s) = a_0 + a_1 s + \sum_{l=1}^{I} b_l K_a(|s-s_l|) \ . \qquad (7)$$

We assume that J sections exist along the t direction, each of which being defined by I data points $P_{ij}(x_{ij}, y_{ij}, z_{ij})$, $1 \le i \le I$. The parametric equations of the J sections are given by expression (7) for the coefficients a_0, a_1 and b_l which are solution of the following linear system:

$$\begin{bmatrix} \cdots & \cdots & \cdots & \cdots & \cdots & | & 1 & s_1 \\ \vdots & \cdots & \cdots & \cdots & \vdots & | & \vdots & \vdots \\ \vdots & \cdots & K_a(|s_i-s_l|) & \cdots & \vdots & | & 1 & s_i \\ \vdots & \cdots & \cdots & \cdots & \vdots & | & \vdots & \vdots \\ \vdots & \cdots & \cdots & \cdots & \vdots & | & 1 & s_I \\ --- & --- & --- & --- & --- & - & - & - \\ 1 & \cdots & 1 & \cdots & 1 & | & 0 & 0 \\ s_1 & \cdots & s_i & \cdots & s_I & | & 0 & 0 \end{bmatrix} \cdot \begin{bmatrix} b_1 \\ \vdots \\ b_i \\ \vdots \\ b_I \\ - \\ a_0 \\ a_1 \end{bmatrix} = \begin{bmatrix} P_{11} & \cdots & P_{1j} & \cdots & P_{1J} \\ \vdots & \cdots & \cdots & \cdots & \vdots \\ P_{i1} & \cdots & P_{ij} & \cdots & P_{iJ} \\ \vdots & \cdots & \cdots & \cdots & \vdots \\ P_{I1} & \cdots & P_{Ij} & \cdots & P_{IJ} \\ - & - & - & - & - \\ 0 & \cdots & 0 & \cdots & 0 \\ 0 & \cdots & 0 & \cdots & 0 \end{bmatrix} . \qquad (8)$$

The notation employed on the right side of equation (8) includes the data points of the J sections considered along the t direction. In fact, the coefficients a_0, a_1, b_i are matrix coefficients, a different set of coefficients being obtained for each section.

Equation (8) can be written in compact form as follows:

$$[K_A] \cdot [b] = [P] \ , \qquad (9)$$

where $[b] = \{b_1 \ldots b_i \ldots b_I \ a_0 \ a_1\}^T$. Solving for $[b]$ gives

$$[b] = [K_A]^{-1} \cdot [P] \qquad (10)$$

and substituting in (7) yields in a compact notation all the equations of the J sections

along the t direction

$$[P_{t_j}(s)]^T = [\cdots K_a(|s-s_I|)\cdots 1\ s\ ]\,[K_A]^{-1}\begin{bmatrix} P_{ij} \\ - \\ \cdots 0 \cdots \\ \cdots 0 \cdots \end{bmatrix}. \tag{11}$$

The parametric equation of a curve in the t direction (with parameter s constant) for a profile B with a linear drift can be written in a similar fashion as follows:

$$P_s(t) = A_0 + A_1\, t + \sum_{k=1}^{J} B_k\, K_b(|t-t_k|) \tag{12}$$

with

$$\begin{bmatrix} \cdots & \cdots & \cdots & \cdots & \cdots & | & 1 & t_1 \\ \vdots & \cdots & \cdots & \cdots & \vdots & | & \vdots & \vdots \\ \vdots & \cdots & K_b(|t_k-t_j|) & \cdots & \vdots & | & 1 & t_j \\ \vdots & \cdots & \cdots & \cdots & \vdots & | & \vdots & \vdots \\ \vdots & \cdots & \cdots & \cdots & \vdots & | & 1 & t_J \\ --- & --- & --- & --- & --- & - & - & - \\ 1 & \cdots & 1 & \cdots & 1 & | & 0 & 0 \\ t_1 & \cdots & t_j & \cdots & t_J & | & 0 & 0 \end{bmatrix} \cdot \begin{bmatrix} B_1 \\ \vdots \\ B_j \\ \vdots \\ B_J \\ - \\ A_0 \\ A_1 \end{bmatrix} = \begin{bmatrix} P_{11} & \cdots & P_{iI} & \cdots & P_{II} \\ \vdots & \cdots & \cdots & \cdots & \vdots \\ P_{1j} & \cdots & P_{ij} & \cdots & P_{Ij} \\ \vdots & \cdots & \cdots & \cdots & \vdots \\ P_{1J} & \cdots & P_{iJ} & \cdots & P_{IJ} \\ - & - & - & - & - \\ 0 & \cdots & 0 & \cdots & 0 \\ 0 & \cdots & 0 & \cdots & 0 \end{bmatrix}. \tag{13}$$

Finally, the equations of the I sections along the s direction are

$$[P_{s_i}(t)]^T = [\cdots K_b(|t-t_k|)\cdots 1\ t\ ]\ [K_B]^{-1} \begin{bmatrix} P_{ij}{}^T \\ - \\ \cdots 0 \cdots \\ \cdots 0 \cdots \end{bmatrix}. \qquad (14)$$

Equations (11) and (14) can be summarised by a general equation, which incorporates in a single formula the kriging equations of the I and J sections for the s and t parameters respectively:

$$P(s,t) = [\cdots K_a(|s-s_i|)\cdots 1\ s\ ]\ [K_a]^{-1} \left[\begin{array}{c|cc} & 0 & 0 \\ P_{ij} & \vdots & \vdots \\ & 0 & 0 \\ \hline 0 \ \ldots \ 0 & 0 & 0 \\ 0 \ \ldots \ 0 & 0 & 0 \end{array}\right]$$

$$[K_B]^{-1} \begin{bmatrix} \vdots \\ K_b(|t-t_k|) \\ \vdots \\ - \\ 1 \\ t \end{bmatrix}. \qquad (15)$$

The above equation yields the parametric representation of a complex surface. The drift and covariance for each kriging profile may be changed: this will affect the shape of the kriged surface. For example when $K(h) = h$, a piecewise linear surface is obtained. It can be demonstrated also that kriging with $K(h) = h^3$ and a linear drift is equivalent to bicubic spline interpolation (**11**). As described in (**14**), this method is well suited to

represent simple as well as complex surfaces.

2.2.3 Surface normal vector

The partial derivatives of Eq. (15) with respect to s and t define two slope vectors on the patch surface. The slope vector of the surface at point $P(s,t)$ in the s direction is

$$\frac{\partial P(s,t)}{\partial s} = \left[\frac{\partial x(s,t)}{\partial s} \quad \frac{\partial y(s,t)}{\partial s} \quad \frac{\partial z(s,t)}{\partial s} \right]^T . \tag{16}$$

Similarly, the slope vector of the surface at point $P(s,t)$ in the t direction is

$$\frac{\partial P(s,t)}{\partial t} = \left[\frac{\partial x(s,t)}{\partial t} \quad \frac{\partial x(s,t)}{\partial t} \quad \frac{\partial z(s,t)}{\partial t} \right]^T . \tag{17}$$

The unit normal vector to the patch surface (see Figure 2.4) at point $P(s,t)$ is a function of the cross-product of these slope vectors (see ref. **(8)**):

$$N(s,t) = \frac{\frac{\partial P(s,t)}{\partial s} \times \frac{\partial (s,t)}{\partial t}}{\left| \frac{\partial P(s,t)}{\partial s} \times \frac{\partial P(s,t)}{\partial t} \right|} . \tag{18}$$

2.3 COMPENSATION PROCEDURE

When measuring objects using a spherically-tipped touch probe on a CMM, the

data obtained are the coordinates of the probe centre when contact occurs. It is then necessary to compensate for the probe radius. This process involves estimating the part surface normal vector $N_{a,i}$ (see Figure 2.1), then compensating the measured points and finally generating the compensated surface. $N_{a,i}$ fulfils the tangential condition of touch for the compensated surface. However since initially we only have the probe tip centre points. The proposed method consists of estimating the part surface normal by the probe centre surface normal (see Figure 2.5). The two normals are in general not equivalent and so a test is proposed later to evaluate the validity of this approximation.

2.3.1 Measurement and generation of the probe centre surface

The measurement data consists of J profiles (in the t direction) of I points (along the s direction) forming a IxJ mesh. The distribution of the points on the profiles need not be regular and so their density can be increased in the most complex regions. When the probe arrives at the end of each path, a new profile can be defined (see Figure 2.6). The surface is then generated by kriging interpolation using specified *drift* and *covariance* values (see Figure 2.3). This surface named S_p is the trajectory surface of the probe centres (using formula (15)). The data have uncertainties and so it could be argued that the generated surface could be allowed to deviate from the points. Kriging allow such fitting technique through the "nugget effect" (13). However since our aim is to use CMMs which have high precision and to use only a minimum number of data points, we have not performed any fitting in our work.

2.3.2 The compensated surface

If $P_{p,i}$ is the *i-th* measured point (probe centre) on the probe centre surface S_p, then the normal vector at $P_{p,i}$, $N_{p,i}$, is calculated using formula (18). So, as shown in Figure 2.5, if R is the radius of the probe, then the offset point on the compensated surface $P_{c,i}$ is simply estimated by

$$P_{c,i} = P_{p,i} + R\, N_{p,i} \,. \tag{19}$$

The compensated surface S_c can now be generated by formula (15) using the $P_{c,i}$ points. The program we have developed to compensate for the probe radius reads the probe centre positions from a raw measurement data file. This file consists of a series of profiles along the surface parameter s or t, each profile containing a equal number of probe centre positions. The offset points are then calculated, saved and finally used to generate the compensated surface (see Figure 2.6).

2.4 EXPERIMENTAL RESULTS

In order to evaluate the proposed method, the following tests were carried out:

1) Measurement of known reference surfaces. - A nominally flat and a nominally spherical part were tested in order to examine the accuracy of surfaces generated by kriging and the correctness of the compensating algorithms. However these tests do not validate fully the approach since for these surfaces a normal to the probe centre surface is also normal to the part surface.

2) Measurement of a free-form surface. - A turbine blade surface was measured with various probe radii in order to estimate the closeness of the compensated surface to the part surface and whether it fulfils the tangential condition of touch.

2.4.1 Test with reference artefacts

Tests were conducted using a moving bridge CMM having a measuring volume of 800 x 700 x 600 mm. Its repeatability 3 μm in x, y and z and its volumetric accuracy is 0.01 μm in accordance with the ANSI B 89.1.12M standard. In order to assess the ability of the proposed method to generate a faithful description of non free-form but known part surfaces, measurements were made on a nominally flat surface of 200 mm x 300 mm and on a sphere of 20 mm diameter of high accuracy. Together with the necessary measurements for the generation of the surfaces, ten randomly distributed points were also probed. The random points were used to verify the validity of the probe centre surfaces. The distances between the random points and the probe centre surface were calculated as well as the distances between the compensated and theoretical surfaces at the grid points. The flat and hemisphere parts were measured using 7 rows of points and 5 points along each row, resulting in a 7 x 5 grid of points. The parametric surface was interpolated to the scanned data by using the kriging algorithm presented in section 3. The root mean square (RMS) error between a set of points and a surface was calculated as follows:

$$\hat{d} = [\ \frac{1}{n} \sum d_i^{\,2}\ ]^{\frac{1}{2}}\ , \qquad (20)$$

where d_i is the shortest distance from a point to the surface. The RMS error calculated between the random points and the probe centre surface was $\hat{d} = 0.0006$ mm for the flat part and 0.0007 mm for the spherical part, thus supporting the kriging algorithms.

For the compensated surface we used the difference between the compensated grid points and the theoretical surfaces. In this case, for the flat part, $\hat{d}$ was 0.0007 mm and for the spherical part, $\hat{d}$ was 0.0013 mm. The results are within the repeatability of the CMM. Figure 2.7 and 2.8 show the surfaces for the flat and the hemisphere. There are no observable instability in the interpolated surfaces.

2.4.2 Test with a free-form surface

The proposed method uses the normal vector to the probe centre surface $N_{p,i}$ in order to generate a point $P_{c,i}$ on the compensated surface. However, in reality during the measurement procedure the tangential condition of touch requires that the probe centre $P_{p,i}$ is located along the normal $N_{a,i}$ to the part surface at the contact point. The following test aims at verifying to what extent the probe centre points and the generated compensated surface fulfil this condition.

As illustrated in Figure 2.9 the generated compensated surface fulfils the tangential condition at probing if point $P_{p,i}^{*}$, as given by Eq. (21), coincides with the probe centre point $P_{p,i}$:

$$P_{p,i}^{*} = P_{c,i} + R \cdot N_{c,i} , \qquad (21)$$

where $N_{c,i}$ is the compensated surface normal at $P_{c,i}$. The experimental verification of this test was performed on a turbine blade shown in Figure 2.10. The blade was measured with three different probe radii ($r=0.5$ mm, $r=1$ mm, $r=2$ mm) using 19 rows of points with 10 points along each row. The points were measured at variable incremental distances depending on the apparent local changes of the surface shape. A parametric surface was interpolated to the probe centre data using kriging interpolation, then the normal vectors $N_{p,i}$ at each position of the probe centre was calculated and the $P_{c,i}$ points were calculated. Three compensated surfaces, one for each probe diameter, were generated using the method described in section 3 (see Figure 2.11). After calculation of the normal vector at each position of the compensated surface $P_{c,i}$, the $P_{p,i}^{*}$ are then calculated and then the shortest distance between $P_{p,i}^{*}$ and probe centre surface are computed using the following equation :

$$e = [\frac{\Sigma D_i^2}{n}]^{\frac{1}{2}}. \qquad (22)$$

Where D_i is the shortest distance between $P_{p,i}^{*}$ *and* $P_{p,i}$. The results of this validation are shown in Table 2.1. It shows that for the present test conditions the compensated surface

fulfils very closely, the tangential condition of touch. However, as the probe radius increases, so does e. This illustrates the importance of selecting a small probe radius provided that the surface finish does not affect the measurement. The error still remains much below the CMM repeatability errors. This test is essential to evaluate whether the use of probe centre normals for compensation purpose is justified given the free-form surface and the probe radius used.

2.5 CONCLUSION

A new method has been proposed, simulated and tested for the digitization of complex surfaces using data acquired with CMM equipped with a spherically-tipped touch trigger probe. Kriging interpolation was used to construct the mathematical equation of the complex surface through the probe centre points initially acquired during the measuring process. The compensation of probe radius can be achieved by determining the normal vectors to this surface at each measured position. Because, in fact, the compensation procedure should be carried out with the normals to the actual surface and not to the probe centre surface, tests have been conducted to verify that the tangential condition of touch was sufficiently fulfilled.

Other experimental validations using flat and spherical surfaces with various probe radii were also conclusive in supporting the high accuracy of this approach. A turbine blade was measured and results showed that the method is accurate to well within the repeatability of the CMM. Therefore this method should greatly assist in the digitization

of free form surfaces for reverse engineering purposes.

Further work is required to assess the minimum number and optimal distribution of measured points to reproduce the actual surface faithfully. Also the proposed method could form the basis of an iterative procedure which adjusts the compensated grid points using residuals provided by the test on the tangential condition of touch. The result would be an unbiased estimate of the workpiece surface. The initial guess for the part surface could be generated as proposed.

References

1 Chen, Y. Free form curve and surface measurement, modelling and machining. *Ph.D. dissertation, the University of Michigan-Ann Arbor*, 1991.

2 Bradley, C., Vickers, G. W. and Milroy, M. Reverse engineering of quadric surface employing three-dimensional laser scanning. *Proc. Instn. Mech. Engrs*, 1994, **208**.

3 Aoyama, H. and Kawa, M. A new method for detecting the contact point between a touch probe and a surface. *Annals of CIRP*, **38**, 1989.

4 Kawabe, S., Kimura, F. and Sata, T. Automatic generation of NC command for 3-D coordinate measuring machines. *Bulletin of the Japan Society of precision Engineering*, 1980, **14**.

5 Lau, K., Duffie, N. and Bollinger, J. Automatic contour measurement for three-dimensional geometry. *Manufacturing Engineering Transactions*, 1985, **13**.

6 Evershim, W. Automatic generation of parts program for CNC-coordinate measuring machines linked to CAD/CAM systems. *Annals of CIRP*, 1986, **33(1)**.

7 Yau, H. T. and Menq, C. H. Path planing for automated dimensional inspection using coordinate measuring machines. *IEEE Robotic and Control Conference Proceedings, (Los Alanitos: IEEE Computer Society Press)*, 1991, **3**.

8 Faux, I. D. and Pratt, M. J. Computational Geometry for Design and Manufacturing. *Elliss Horwood Publishers*, 1980.

9 Gilbert, R., Carrier, R., Benoit, C., Soulie, M. and Schiette-Katte, J. Application of dual kriging in human factors engineering. *Advances in Industrial Ergonomics and Safety II, (Biman Das, Editor)*, Taylor & Francis, London, 1990.

10 Krige, D. G. A Statistical approach to some basic mine valuation problems on the witwatersrand. *J. Chem. Metal. Min. Soc. S. Afr.*, 1951, **S2**.

11 Matheron, G., The intrinsic random functions and their applications. *Adv. Appl. Prob.*, 1973, **5**.

12 Matheron, G. Splines et krigeage: leur équivalence formelle. *Rapport N-667, Centre de Géostatistique, Fontainebleau, École des Mines de Paris*, 1980.

13 Trochu, F. A contouring program based on dual kriging interpolation. *Engineering with computers*, 1993, **9**.

14 Trochu, F. and Larocque, S. Présentation d'un logiciel de modélisation géométrique par krigeage dual. *Huitième Congrès Canadien de l'éducation en ingénierie*, 1992.

Table 2.1 RMS value of the distance between the measured and predicted probe centre points calculated from the compensated surface.

Probe radius(mm)	e(mm)
r=0.5	0.000044
r=1.0	0.000164
r=2.0	0.000756

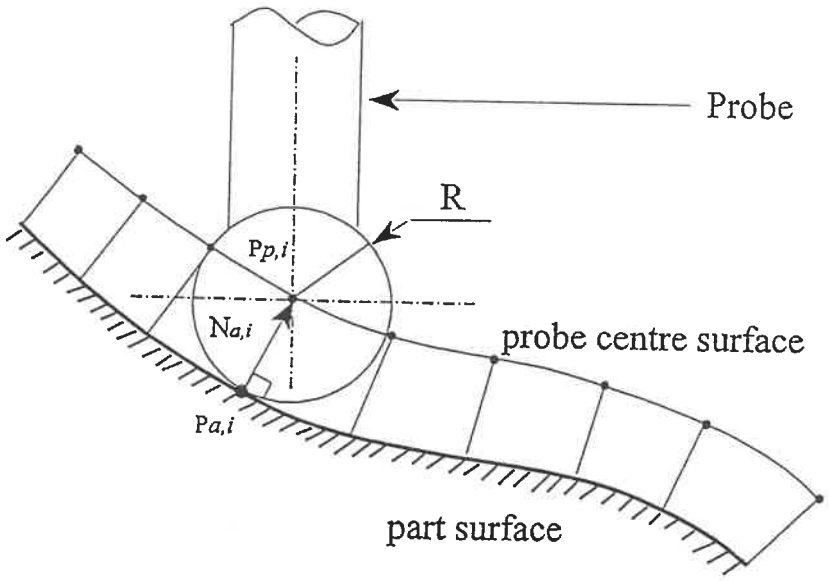

Figure 2.1 The tangential condition between the touch probe and the part.

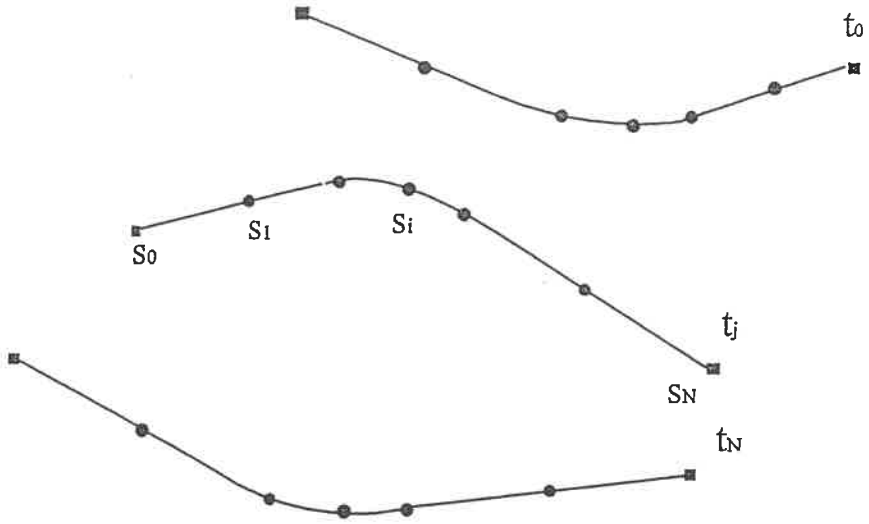

Figure 2.2 2D curves used to generate a 3D surface.

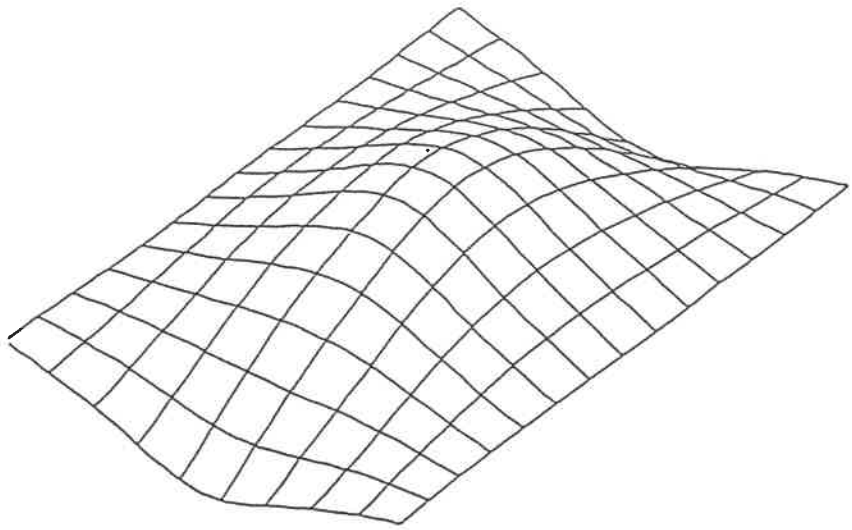

Figure 2.3 Sculptured surface generated using kriging.

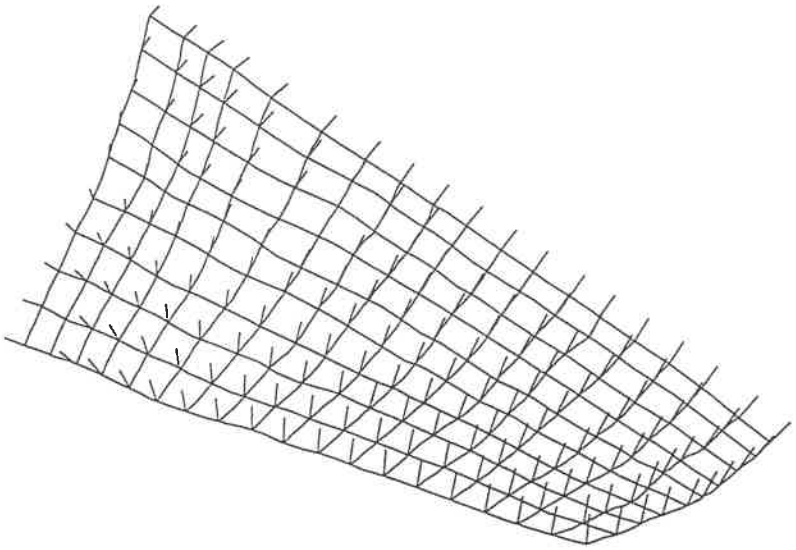

Figure 2.4 Probe centre surface with its normal vectors.

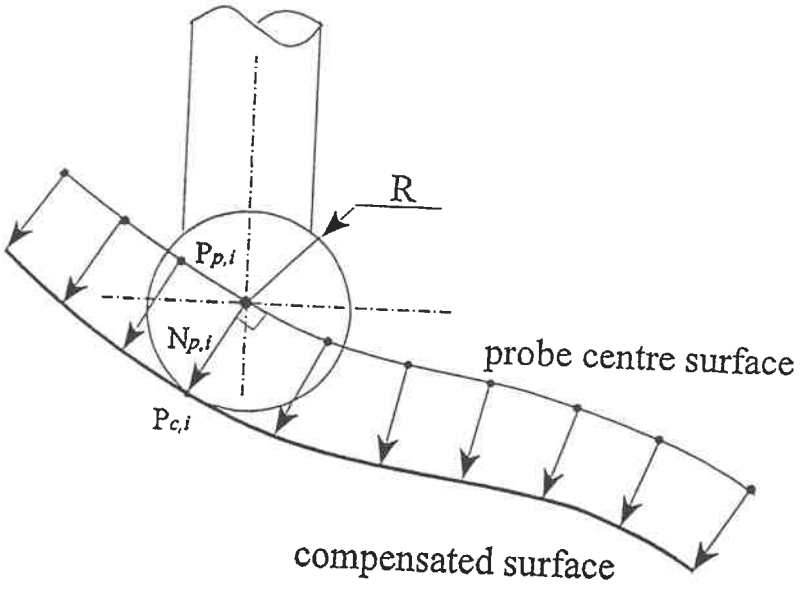

Figure 2.5 The compensation of the probe centre points using the probe centre surface normals.

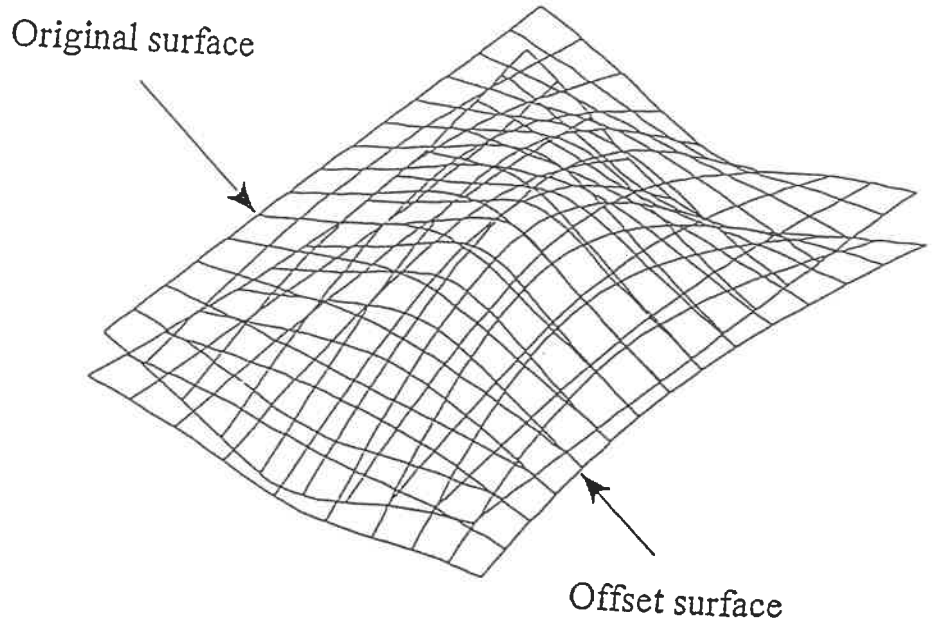

Figure 2.6 Original and offset surface.

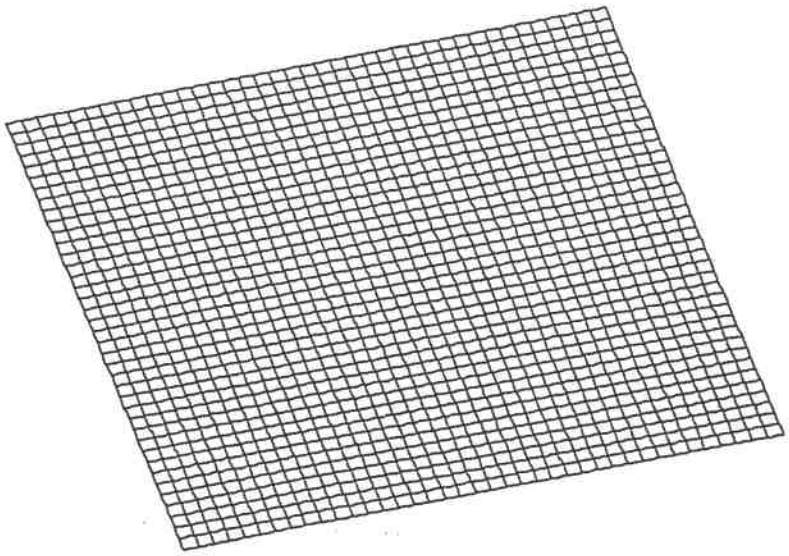

Figure 2.7 Compensated surface geenrated for a flat part.

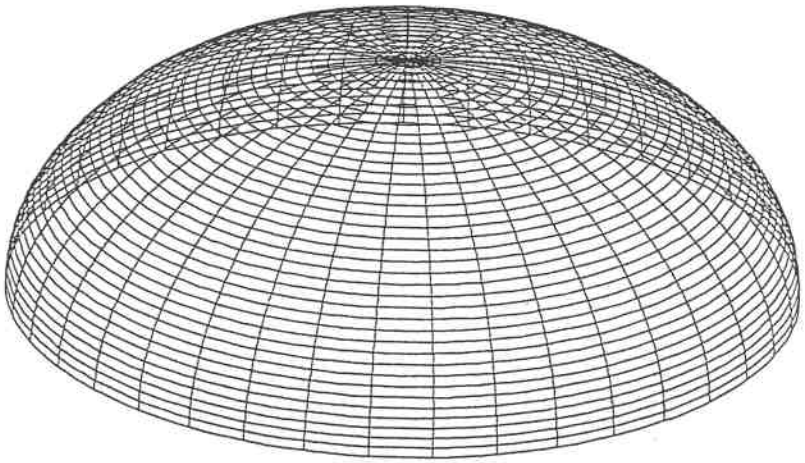

Figure 2.8 Compensated surface generated for a hemisphere.

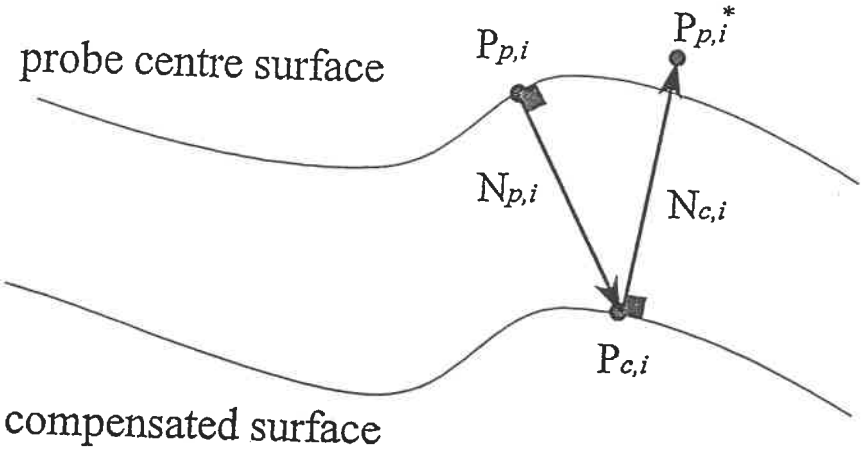

Figure 2.9 The relationship between the measured probe centre ($P_{p,i}$), the compensated point ($P_{c,i}$) and predicted probe centre point($P_{p,i}^{*}$) based on the tangential condition of the touch.

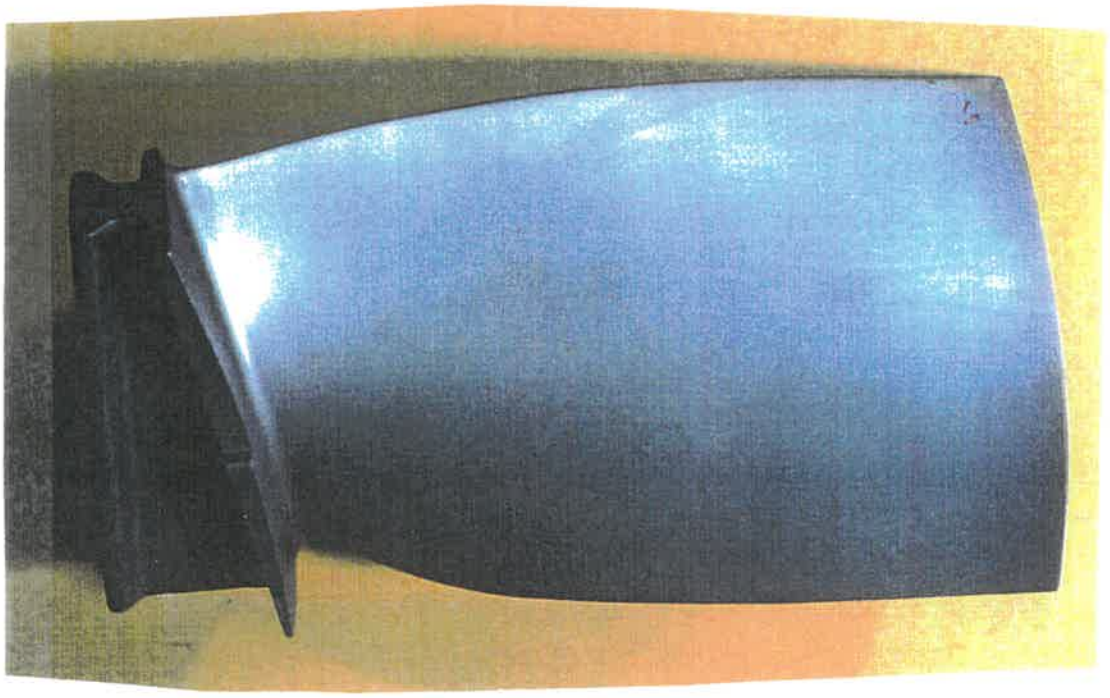

Figure 2.10 Turbine blade used for evaluating the method.

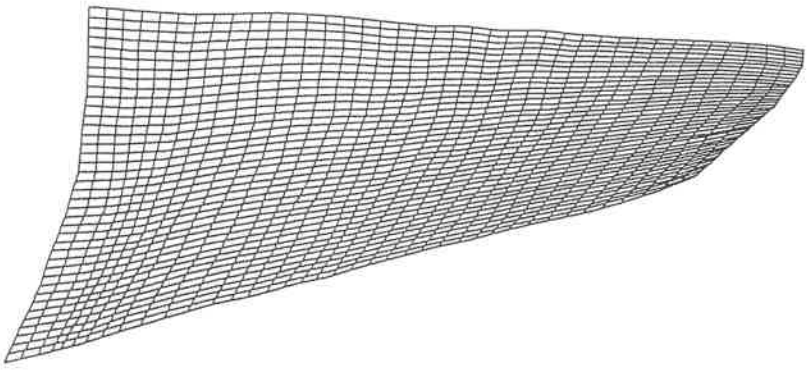

Figure 2.11 Compensated surface generated for a turbine blade.

Chapter 3

Paper 2

"Adaptive Measurement Strategy of Unknown Sculptured Surfaces on a Coordinate Measuring Machine"

paper written by Y. A. Mir, J. R. R. Mayer and M. Balazinski and submitted to the *Journal of Design and Manufacturing*.

Abstract

A new method for the programming of coordinate measuring machine to measure unknown sculptured parts and surfaces is described in this paper. Several points on an actual surface are initially measured under manual control with the CMM. An initial surface is then generated using these initial points with a kriging modeller. The reliability of this initial surface is gradually improved by progressively adding measurement points. The new target points used to drive the CMM are selected on the basis of the local complexity of the current estimate of the part surface to produce an accurate and rapid result. Experimental results indicate that the developed method is able to create a useful program providing a model accurate within a given tolerance in a minimum time.

Keywords: Coordinate measuring machine, machine programming, measurement, reverse engineering

3.1 INTRODUCTION

In recent years, 3D coordinate measuring machines (CMMs) have become the primary equipment for the quality control and digitization of sculptured surfaces. Sculptured surfaces can be seen in many modern mechanical parts such as turbine blades, advanced aerodynamic shapes used in today's car bodies, in the aircraft industry etc. As the workpiece has become more complex, their digitization with a CMM has become more difficult and time consuming. Since inspection time, cost and measurement precision depend on good inspection planning and CMM performance, an adaptive measuring strategy has been developed to ensure an accurate and rapid digitization of unknown sculptured surfaces.

To ensure an accurate digitization, several conditions must be fulfilled: (1) Probe compensation must be done along the normal of the surface at the point of contact between the probe tip and the surface; (2) The probe radius must be adapted to the surface condition; (3) an appropriate sampling interval must be estimated, especially in the case of a complex surface.

When measuring an object with a CMM, the coordinates of the probe centre P are initially measured by the CMM controller (see Figure 3.1). To calculate the exact coordinate of the contact point $\mathbf{M}'$ between the probe and the object, the normal vector $\mathbf{N}'$ of the surface at the contact point has to be known. If $\mathbf{N}'$ is not known and is

replaced by the probe approach vector N, a measurement error will result from the angular error $\Delta \alpha$. A number of methods have already been proposed to address this problem. The first method uses a new touch probe which can directly detect the contact point between the surface and the probe. Aoyama and Kawa (1989), developed such a touch probe based on a spherical potentiometer. This hardware method requires complex and accurate mechanisms and it remains very difficult to make small probes with fine discrimination at a reasonable cost. The second method uses the nominal CAD model of the part and finds the normal direction at the point to be measured, so that the approach direction is along the surface normal (Kawab, 1980; Lau et al, 1985; Evershim, 1986; Yau et al 1991). The limitation of this method is that the part geometry information is required. Another drawback is the necessity to approach the surface along its normal which requires a minimum clearance distance. Also this precludes the use of scanning routine, which are much faster and which do not use a normal approach. The third method is used when no CAD model is available. First the generation of a compensated surface from measured probe centre point is required. Here the normal vector at each measured point is calculated from a surface model based at the measured probe centre coordinates. Then each point is displaced by one probe radius r, in the direction of the normal. The surface generated from the compensated points will be the measured surface (Mayer et al, 1995). This method is used to measure complex free form surfaces and it increases the potential use of CMMs in reverse engineering applications.

A very time-consuming task in programming a CMM is defining the probing

points and trajectory points for unknown feature measurement. In this paper a new approach that can create rapidly and automatically a programme for digitizing an unknown sculptured surface is proposed. A precise mathematical model is used to represent a sculptured surface and an adaptive measurement scheme is used to obtain a set of precise target points to finalize the digitizing procedure. Since an actual part is used, the approach is applicable to reverse engineering, for the construction of a model from an existing specimen.

This paper is divided into five sections. Section 1 contains the problem description and some introductory remarks. Section 2 describes a mathematical model for the representation of complex surfaces. The adaptive measurement strategy is presented in section 3. Section 4 presents an experimental validation, followed by concluding remarks.

3.2 SURFACE GENERATION

Generally, free form sculptured surfaces cannot be represented in simple analytic forms. Therefore, they are defined in a piecewise fashion; i.e. a surface is composed of a number of segments (patches) which are jointed together with some specified continuity conditions. Ferguson (1964) first introduced the use of parametric cubic equations and blending functions for aircraft design, and Coons (1967) established the solid modelling by introducing nonlinear polynomials and bicubic surface interpolating techniques to represent surface patches. However, their method requires a great deal of mathematical information and calculation to define surfaces, and it has certain

disadvantages when the shape of the surface needs to be changed or controlled. Bezier (1972) developed the UNISURF system to design the sculpture surfaces of automobile bodies based on the Berstein polynomials. This system allows easy shape control of surfaces in a predictable way by changing a few simple parameters, called the control points. However, local changes in a Bezier surface tend to strongly propagate throughout the entire surface. Riesenfield (1973) further advanced the local control property of surfaces by using B-splines.

In this study, a method called Kriging is used for the construction of a surface of which the Bezier and the B-splines methods are subsets. Surface kriging is a new method for the representation of sculptured surfaces (Faux and Pratt, 1980 ; Krige, 1951 ; Matheron, 1973; Matheron 1980). It was first proposed by Gilbert et al (1990). It is presented in a more general framework by Trochu et al (1992), who applied the method to model various types of surfaces. It has two main advantages: (1) *Its accuracy*, because the surface is represented by a continuous and differentiable parametric equation ; (2) *Its generality*, because piecewise linear, "B-spline" and Bézier surfaces are particular cases of kriging and least square methods can be derived as a limit case (Trochu, 1993). Another advantage of kriging concerns the determination of the normal vectors at any point of the surface, which can be computed exactly from the kriged mathematical equation of the surface. A formal description of parametric surface kriging now follows.

3.2.1 Parametric surface

A three-dimensional surface is described by a parametric equation of the form $\boldsymbol{P} = \boldsymbol{P}(s,t)$, with component functions $x = x(s,t)$, $y = y(s,t)$, $z = z(s,t)$. A parametric surface is defined by two kriging profiles A and B along the s and t directions respectively. A kriging profile consists of a drift and a generalized covariance which govern the shape of the surface. The parametric equations of a curve in the t direction for a kriging profile with a linear drift and a generalized covariance $K_a(h)$ can be written as follows :

$$P_t(s) = a_0 + a_1 s + \sum_{l=1}^{I} b_l K_a(|s-s_l|) \qquad (1)$$

Where the coefficients a_0 , a_1 and b_l are vector coefficients. We assume that J sections exist along the t direction, each section being defined by I data points $P_{ij}(x_{ij}, y_{ij}, z_{ij})$, $1 \leq i \leq I$. The parametric equations of each of the J sections are given by equation (1) and the coefficients a_0, a_1 and b_l are solutions of the following linear system which uses the known values of the data points :

$$\begin{bmatrix} \cdots & \cdots & \cdots & \cdots & \cdots & | & 1 & s_1 \\ \vdots & \cdots & \cdots & \cdots & \vdots & | & \vdots & \vdots \\ \vdots & \cdots & K_a(|s_i-s_l|) & \cdots & \vdots & | & 1 & s_i \\ \vdots & \cdots & \cdots & \cdots & \vdots & | & \vdots & \vdots \\ \vdots & \cdots & \cdots & \cdots & \vdots & | & 1 & s_I \\ --- & --- & --- & --- & --- & - & - & - \\ 1 & \cdots & 1 & \cdots & 1 & | & 0 & 0 \\ s_1 & \cdots & s_i & \cdots & s_I & | & 0 & 0 \end{bmatrix} \cdot \begin{bmatrix} b_1 \\ \vdots \\ b_i \\ \vdots \\ b_I \\ - \\ a_0 \\ a_1 \end{bmatrix} = \begin{bmatrix} P_{1j} \\ \vdots \\ P_{ij} \\ \vdots \\ P_{Ij} \\ - \\ 0 \\ 0 \end{bmatrix} \qquad (2)$$

The notation employed on the right hand side of equation (2) includes the data points of

the J sections considered along the t direction. Note that, a different set of coefficients a_0 , a_1 and b_i is obtained for each of the J section.

Equation (2) can be written in a more compact form as follows :

$$[K_A]\cdot[b]=[P] \tag{3}$$

where [b] = $\{b_1 \ldots b_i \ldots b_I\ a_0\ a_1\ \}^T$. Solving for [b] gives

$$[b] = [K_A]^{-1} \cdot [P] \tag{4}$$

and substituting from (1) yields

$$[P_{t_j}(s)]^T = [\cdots K_a(|s-s_i|)\cdots 1\ s\ ]\ [K_A]^{-1} \begin{bmatrix} P_{ij} \\ - \\ \cdots 0 \cdots \\ \cdots 0 \cdots \end{bmatrix} \tag{5}$$

The parametric equation of a curve for a profile B with a linear drift and a generalized covariance $K_b(h)$ can be written in a similar fashion as follows :

$$P_s(t) = A_0 + A_1\ t + \sum_{k=1}^{J} B_k\ K_b(|t-t_k|) \tag{6}$$

with

$$\begin{bmatrix} \cdots & \cdots & \cdots & \cdots & \cdots & | & 1 & t_1 \\ \vdots & \cdots & \cdots & \cdots & \vdots & | & \vdots & \vdots \\ \vdots & \cdots & K_b(|t_j - t_k|) & \cdots & \vdots & | & 1 & t_j \\ \vdots & \cdots & \cdots & \cdots & \vdots & | & \vdots & \vdots \\ \vdots & \cdots & \cdots & \cdots & \vdots & | & 1 & t_J \\ --- & --- & --- & --- & --- & - & - & - \\ 1 & \cdots & 1 & \cdots & 1 & | & 0 & 0 \\ t_1 & \cdots & t_j & \cdots & t_J & | & 0 & 0 \end{bmatrix} \cdot \begin{bmatrix} B_1 \\ \vdots \\ B_j \\ \vdots \\ B_J \\ - \\ A_0 \\ A_1 \end{bmatrix} = \begin{bmatrix} P_{i1} \\ \vdots \\ P_{ij} \\ \vdots \\ P_{iJ} \\ - \\ 0 \\ 0 \end{bmatrix} \tag{7}$$

Finally, the equations of the I sections along the s direction are

$$[P_{s_i}(t)]^T = [\cdots K_b(|t - t_k|) \cdots 1 \; t] \, [K_B]^{-1} \begin{bmatrix} P_{ij}^{\;T} \\ - \\ \cdots 0 \cdots \\ \cdots 0 \cdots \end{bmatrix} \tag{8}$$

Equations (5) and (8) can be merged into a single general equation, which incorporates the kriging equations of the I and J sections for the s and t parameters respectively (Trochu and Larocque, 1992) :

$$P(s,t) = [\cdots K_a(|s-s_i|)\cdots 1 \; s \;] \; [K_A]^{-1} \left[\begin{array}{c|cc} & 0 & 0 \\ P_{ij} & \vdots & \vdots \\ & 0 & 0 \\ \hline 0 \;\ldots\; 0 & 0 & 0 \\ 0 \;\ldots\; 0 & 0 & 0 \end{array}\right] \cdot$$

$$[K_B]^{-1} \begin{bmatrix} \vdots \\ K_b(|t-t_k|) \\ \vdots \\ 1 \\ t \end{bmatrix} \qquad (9)$$

The above equation yields the parametric representation of a complex surface. The drift and covariance of each kriging profile may be changed: this will affect the shape of the kriged surface correspondingly. For example when $K(h) = h$, a piecewise linear surface is obtained. It can be demonstrated also that kriging with $K(h) = h^3$ and a linear drift is equivalent to bicubic spline interpolation (Matheron, 1973). The method is well suited to represent simple as well as complex surfaces (see Figure 3.2).

3.2.2 Surface normal vector

The surface normal vector will be used to program the probe tip approach direction and to compensate the probe tip diameter. It is easily calculated from the kriged surface. The partial derivatives of Eq. (9) with respect to s and t define two slope vectors on the patch surface. The slope vector of the surface at point $\vec{P}(s,t)$ in the s

direction is

$$\frac{\partial \vec{P}(s,t)}{\partial s} = \left[\frac{\partial x(s,t)}{\partial s} \quad \frac{\partial y(s,t)}{\partial s} \quad \frac{\partial z(s,t)}{\partial s} \right]^T \tag{10}$$

Similarly, the slope vector of the surface at point $\vec{P}(s,t)$ in the t direction is

$$\frac{\partial \vec{P}(s,t)}{\partial t} = \left[\frac{\partial x(s,t)}{\partial t} \quad \frac{\partial x(s,t)}{\partial t} \quad \frac{\partial z(s,t)}{\partial t} \right]^T \tag{11}$$

The unit normal vector to the patch surface (see Figure 3.3) at point $\vec{P}(s,t)$ is the normalised cross-product of these slope vectors :

$$\vec{N}(s,t) = \frac{\frac{\partial \vec{P}(s,t)}{\partial s} \times \frac{\partial (s,t)}{\partial t}}{\left| \frac{\partial \vec{P}(s,t)}{\partial s} \times \frac{\partial \vec{P}(s,t)}{\partial t} \right|} \tag{12}$$

3.3 PROPOSED ADAPTIVE MEASUREMENT STRATEGY

In the proposed approach the coordinates of several points on the object are initially measured, under manual CMM control. Then a surface is generated from these compensated measured points. This surface is an approximative representation of the object. The proposed algorithm then calculates a set of points named "target points" and their normal vectors from the estimate surface. These points are then used for further

measuring the object. During digitization the touch probe traverses in the direction of the normal vector towards the target point. Upon contact of the probe with the object, the compensated coordinates of the contact points are recorded. Then, a new surface is constructed using these additional coordinates. This surface is a better estimate of the actual surface. The above procedure continues until the difference calculated between the measured and the target points becomes smaller than a given tolerance. Figure 3.4 shows a schematic diagram of the proposed adaptive method.

3.3.1 Generation of an initial surface using manually measured point

Initially several points are measured on the object using the touch probe. The number and location of the initial points is very important because the surface generated from these points should represent the overall shape of the object surface. For example the number of points in irregular areas should be more than that of smoother areas. These measurements are automatically compensated. A compensated point is given by the probe centre coordinates; offset by one tip radius in a certain direction. In the case of an unknown surface this compensation is in the direction of the closest measurement plane (*xy, yz, xz*) because the surface normal is not known. This introduces errors in the measurement as illustrated in Figure 3.1. As explained in section 2, the surface will be generated using these measured points and Eq. 9. For the generation of the surface it is preferable to use control points in each direction. This process controls the correctness of the surface profiles.

3.3.2 Calculation of the target points

The target points (see Figure 3.5) are used to measure the object and are located on the generated surface. They are a set of points where the touch probe is expected to contact the surface. The components of a target point include its coordinates and normal vector to the surface. During the measurement, the touch trigger probe moves along the normal direction towards the target point. The measured coordinates are then those of the probe ruby centre at contact time, compensated by the ruby radius along the surface normal towards the surface.

A target point is defined by its *s* and *t* parameters, each varying from 0 to 1. For example the coordinates of points representing the four corners of a surface are: *p(0,0), p(0,1), p(1,0), p(1,1)*. The approach will produce the coordinates of all arbitrary points and their normal vectors on the generated surface.

3.3.2.1 Generation of the target points

Two methods can be considered for the generation of the target points : **1)** regular generation of target points ; **2)** irregular generation of target point. The first method, generates a set of uniformly distributed target points on the generated surface. This approach is not efficient since it takes no account of the local complexity of the surface. For the second method, the local complexity of the generated surface is considered and so more points are planned in more complex regions. In order to support this process it is necessary to calculate the tangent and curvature at each previously

measured point.

The tangent and curvature at a point P_1 in a curve is approximated using three points (see Figure 3.6) in the plane and solving for the circle which passes through these three points. The curvature is approximated by the radius of the calculated circle and the tangent is approximated by the tangent to the circle at P_1 . The tangent and curvature of the orthogonal curve are determined in a similar manner. For these approximations to be accurate the five points must be measured accurately and the radius of curvature must exist and be constant across the measured points. The constant curvature requirement is achieved by making the distance between the measured points small compared to the radius of curvature.

The curvature at point P_1 is approximated using one of two methods. For the first method, the three points in the plane are used to define a circle which passes through them (see Figure 3.6-a). The curvature k at P_1 is approximated by the curvature of the circle, i.e., the inverse of the circle radius, R. For the second method, the curvature is approximated by the ratio of the change in the tangent angle and the change in arc length, Figure 3.6-b (Faux and Pratt, 1980).

The second method, uses three consecutive points. By definition, for the 2D case, the curvature is instead given by

$$k=\left|\frac{d\theta}{dv}\right| \tag{13}$$

where θ is the angle between the curve's tangent and the horizontal or x axis. The approximated equation is

$$k\approx\left|\frac{\theta_1-\theta_2}{\Delta v}\right| \tag{14}$$

where $\theta_1=\arctan(\frac{z_1-z_0}{x_1-x_0})$, $\theta_2=\arctan(\frac{z_1-z_2}{x_1-x_2})$ and $\Delta v = \sqrt{(x_1-x_2)^2+(z_1-z_2)^2}$.

The tangent or slope, m, of the curve at point P_1 follows directly from the equations used to determine the curvature.. For the second method, the slope can be approximated as the slope of the line passing through points P_0 and P_2 , i.e.,

$$m=\frac{z_0-z_2}{x_0-x_2} \tag{15}$$

The complexity of a region is defined as the rate of change in the slope, Δm (see Figure 3.6-c). The generation of the target points in a local complex area at each iteration is performed as follows (see Figure 3.7). First, the total curvature of each curve is calculated as the sum of all the calculated Δm for that curve (see Figure 3.8). Then the curve with the largest total curvature is selected. Then on this selected curve, the Δm of each region is calculated. The potential error due to incorrect ruby compensation increases in the region with more complexity. On the basis of a given acceptable measurement error, we can calculate the maximum deviation ($\Delta \theta_{max}$) of

the probe direction from the local surface normal direction (see Figure 3.9). An equivalent acceptable maximum slope variation Δm can then be calculated:

$$\sin(\Delta\theta_{max}) = \frac{BC}{AB}$$
$$\tan(\Delta\theta_{max}) = \frac{AB}{r} \qquad (16)$$

Where $\Delta m=|m_1-m_2|$, $\Delta \theta=|\theta_1-\theta_2|$, BC the acceptance error and r is the ruby radius. For example with a ruby radius of 0.5 mm and an acceptance error of 0.005 mm, the Δm_c is 0.1.

To avoid the problem of error compensation in the complex region, when $\Delta m > \Delta m_c$ a set of three equidistant points added. The s and t parameters of the new points are calculated as follows. If s_{p1}, t_{p1}, ... and s_{p4}, t_{p4} are the s and t values of existing points and $\Delta s=\frac{s_{p1}-s_{p4}}{n+1}$, where n is the number of point which should be added, then the s value of the three new points (s_{q1}, s_{q2}, s_{q3}) are :

$$s_{q1}=s_{p1}+\Delta s \ , \ s_{q2}=s_{p2}+\Delta s \ , \ s_{q3}=s_{p3}+\Delta s \qquad (17)$$

3.3.3 Measuring the part using the target points

Apart from the initial manual measurement of the part, all subsequent measurements are accomplished in computer control mode on the basis of the target points and their surface normal. Figure 3.10 illustrate the process of measuring the target points.

At first relatively large error are expected between the target and the measured points. Also, this may lead to the local normal at the actually measured point to differ from the target point normal. This means that a small error is introduced into the compensation of that measured point. For this reason, all the target points are re-measured at each iteration. A more efficient procedure will be proposed later.

3.3.4 Comparison of the measured and the target points

Because the measured points are the only information about the actual surface, they are the reference for the generated surface. Two tests are used 1) comparison between the measured points and the target points; 2) comparison between the measured points and the generated surface. The root mean square value is used to quantify both criteria. Based on

$$d_{RMS} = [\ \frac{1}{n} \sum d_i^2\ ]^{1/2} \qquad (18)$$

this *RMS* value, a decision can be taken to see whether or not the procedure needs to be repeated. If the results taken from Eq. 18 is out of a specified tolerance, a new surface is generated using the new points. Then steps 3.2 to 3.4 are repeated(see Figure 3.4). As the complexity of the object increases and depending on the initial measured points, the number of iterations will increase.

3.4 VALIDATION

To check the validity of the proposed method, an automatic vector measurement

command has been used. The command causes the CMM to move along a defined vector from a fixed stand off distance along the surface normal in the direction of the target point until it contacts the object. Upon contact, probe compensation is applied along the defined vector then the command outputs the coordinates of the point, and the difference between the target and the measured point.

A porcelain vase of dimensions 200x115x115 mm, was placed on the CMM table . The part was digitized with an LK G90C 8.7.6 CMM using a TP2 touch trigger probe with a ruby of 0.5 mm radius. Initially, 12 (4 rows and 3 columns) points were measured manually as shown in Figure 3.11. An initial surface was then generated, using the 12 grid points. After generating the surface, a set of target points, 7 in s and 5 points in t, were calculated. Having verified that the collected points were on the generated surface a program was created. Then, the CMM measured the object automatically and recorded the coordinates of the contact points. A new surface was generated from the new measured point, with 7 rows, 5 columns (35 grid points). Table 3.1 shows the geometry information of the various iterations and Figure 3.11 shows the additional points at each iteration.

In order to reach a decision on when to stop the iteration procedure, it is necessary to calculate the error between the target and the measured points and between the measured points and the previously generated surface. Actual results are shown in Table 3.2. The RMS distance (d_{RMS}) in each iterations are compared with the accepted

value of repeatability for the CMM (0.003 mm). The final surface generated with a 16 x 5 grid of measured points is shown in Figure 3.12.

As shown in Table 3.2 the procedure was repeated 4 times, and each time the accuracy increased. The time consummation for the above work has been reduce 40% as compare with digitizing of part to achieved the same precision with manual method and also the accuracy of digitizing increase relative to its manual procedure.

An inspection program was written that applies all the necessary commands and steps to perform the complete measurement procedure, including the probe qualification procedure, alignment procedure, touch probe movement etc.

3.5 CONCLUSION AND FUTURE WORK

In this study, a new approach is proposed for the rapid and automatic digitization of unknown complex surfaces using data acquired by a CMM equipped with a spherical tip touch probe. An initial surface is generated from a few points which are manually measured. Then a set of target points are produce which can be used to re-measure the part surface with a higher degree of accuracy. The measurement procedure can be continued until the difference between the measured points and the model becomes smaller than a given tolerance.

The digitization process and its planning are performed automatically. The

benefits of the approach, for the measurement of objects with a CMM and a touch probe, are:

1- Rapid and automatic programming for digitizing complex surfaces.

2- The possibility to digitize unknown sculptured and free form surfaces as encountered in reverse engineering.

3- Measured time can be significantly reduced.

4- The accuracy of the model can be increased as needed.

As mentioned previously, the use of compensated points leads to inefficiencies in the digitization procedure. A more attractive solution consists in recording tip centre points. These points are in effect always valid and can be re-used at each subsequent iterations, by simply changing the ruby compensation direction. However, the target point selection will take place according to the usual scheme for new points but not for already measured points. For these, the target point will have an additional selection constraint. For example it may be that the point is that on the generated surface which is closest to the centre measured coordinates. This approach is undergoing trials.

Acknowledgments

The authors wish to thank Dr. F. Trochu for the kind use of his extensive library of kriging functions. In particular J.R.R. Mayer is grateful to the National Sciences and Engineering Council of Canada for an Individual Research Grant No.OGP0155677.

References

Aoyama H., and Kawa M. (1989) A new method for detecting the contact point between a touch probe and a surface, *Annals of CIRP*, 38, 517-520

Bezier, P. (1972) *Numerical Control*, New York: Wiley.

Coons, S. A. (1967) Surface for computer aided design of space forms. *Report MAC-TR-41 Project MAC (Cambridge, MA: MIT).*

Evershim, W. (1986) Automatic generation of parts program for CNC-coordinate measuring machines linked to CAD/CAM systems. *CIRP Annals*, 33 (1).

Faux, I. D., Pratt, M. J. (1980) *Computational Geometry for Design and Manufacturing*, Elliss Horwood Publishers.

Ferguson, J. C. (1964) Multivariate curve interpolation. *Journal ACM*, 11, 221-228.

Gilbert, R., Carrier, R., Benoit, C., Soulie, M., Schiette-Katte, J. (1990) Application of dual kriging in human factors engineering. *Advances in Industrial Ergonomics and Safety II, (Biman Das, Editor), Taylor & Francis, London.*

Kawabe S. et al (1980) Automatic generation of NC command for 3-D coordinate measuring machines. *Bulletin of the Japan Society of precision Engineering*, 14, 177-8.

Krige, D. G. (1951) A statistical approach to some basic mine valuation problems on the witwatersrand. *J. Chem. Metal. Min. Soc. S. Afr.*, S2, 119-139.

Lau, K., Duffie, N. and Bollinger, J. (1985) Automatic contour measurement for three-dimensional geometry. *Manufacturing Engineering Transaction,* (13), 535-540.

Matheron, G. (1973) The intrinsic random functions and their applications. *Adv. Appl Prob.* 5, 439-468.

Matheron, G. (1980) Splines et Krigeage: leur équivalence formelle. *Rapport N-667, Centre de Géostatistique, Fontainebleau, École des Mines de Paris.*

Mayer, J. R. R., Mir, Y. A., Balazinski, M., Trochu, F., Vafaeesefat, A. (1995) Modelling of sculptured surface from touch probe measurements. *Accepted to the Concurrent Engineering Conference August 1995.*

Riesenfield, D. F. (1973) Application of b-splines approximation to geometric problems of computer aided design. *PhD Thesis Syracuse University.*

Trochu, F., Larocque, S. (1992) Présentation d'un logiciel de modélisation géométrique par krigeage dual. *Huitième Congrès Canadien de L'éducation en Ingénierie*, 279-295.

Trochu, F. (1993) A contouring program based on dual kriging interpolation. *Engineering with Computers*, Vol 9, 160-177.

Yau, H. T. and Menq, C. H. (1991) Path planing for automated dimensional inspection using coordinate measuring machines. *IEEE Robotic and Control Conference Proceedings,(Los Alanitos: IEEE Computer Society Press)*, 3, 1934-1939.

Table 3.1 Geometry information of the generated surface of each procedure

Iteration	Number of points in s direction	Number of points in t direction	Number of grid points	Symbol on the Fig. 10	Number of control points
initial	4	3	12	○	40 x 30
1	7	5	35	○	50 x 40
2	10	5	50	■	55 x 40
3	13	5	65	□	60 x 40
4	16	5	80	★	65 x 40

Table 3.2 The result of procedure evaluation.

Iteration	*d(TP,PGS)* (mm)	*d(PGS,MP)* (mm)	*d(TP,MP)* x(mm)	y(mm)	z(mm)	*n*	*EC* (mm)	*CP*
Initial	---	---	---	---	---	12	---	---
1	0.000445	1.885	0.686	1.107	1.434	35	1.882	*Y*
2	0.000324	0.021	0.014	0.019	0.018	50	0.018	*Y*
3	0.000196	0.006	0.004	0.009	0.007	65	0.003	*Y*
4	0.000101	0.003	0.002	0.002	0.003	80	0.000	*N*

Where:
TP= Targets Points,
PGS= Previously Generated Surface,
MP= Measured points,
n= number of points on the surface,
EC= Error Calculated,
CP= Continue Procedure, *Y*= Yes, *N*=No,
d(TP,MP)= distance calculated between *TP* and *MP*,
d(PGS,MP)= distance calculated between *PGS* and *MP*.

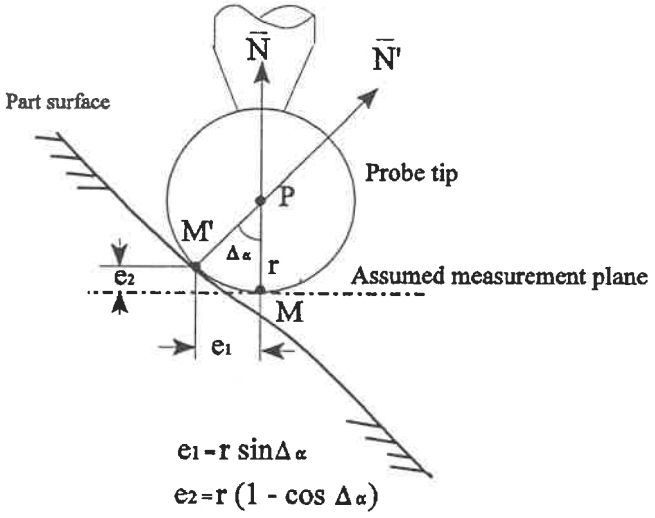

Figure 3.1 Measurement errors resulting from an incorrect surface normal vector.

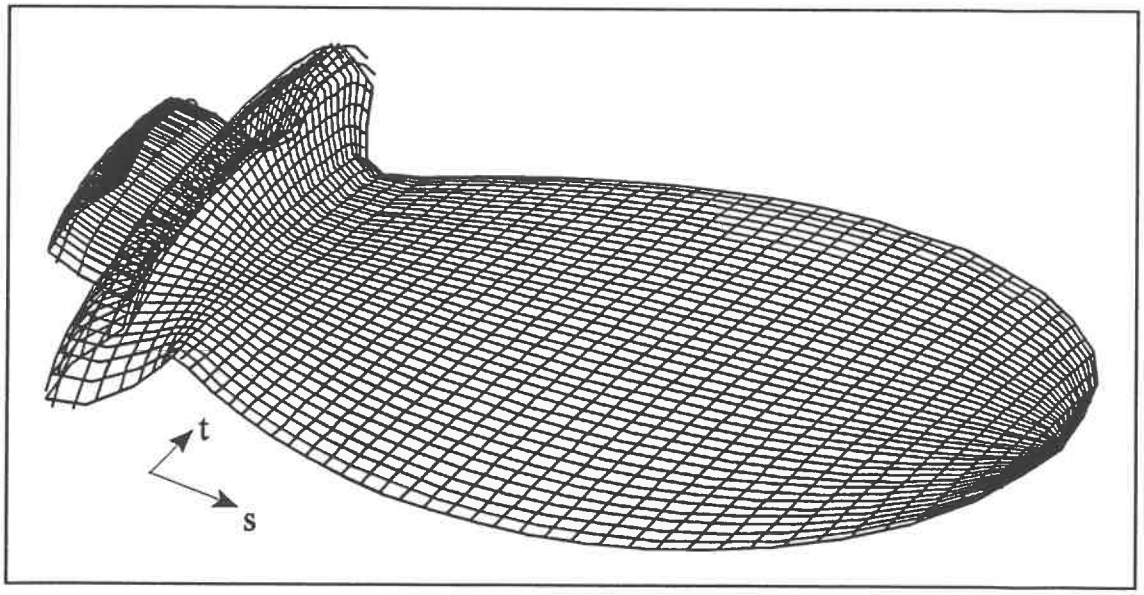

Figure 3.2 A sculptured surface generated using the Kriging method.

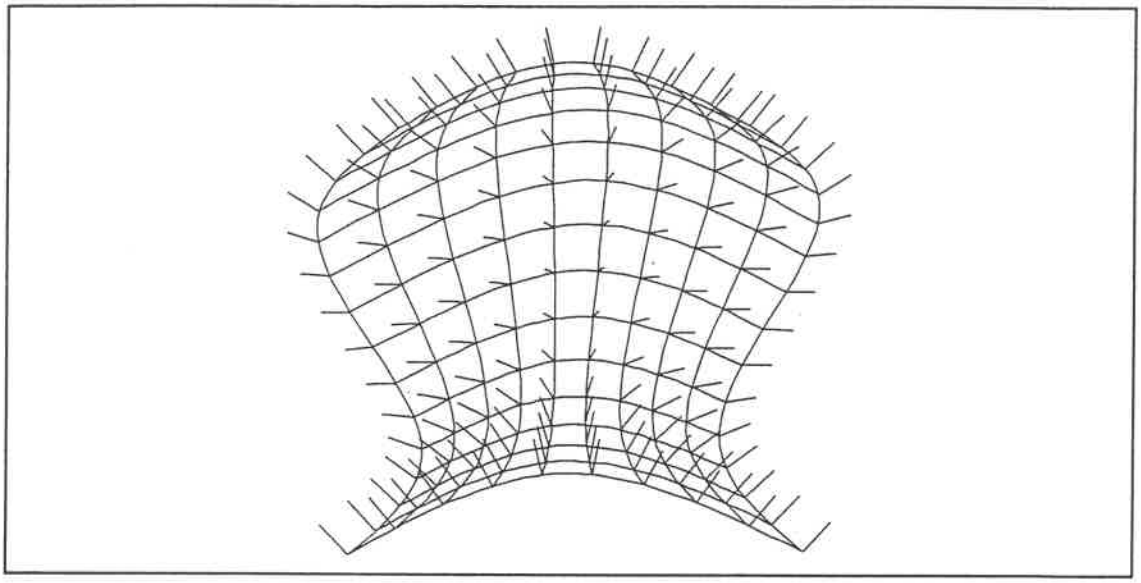

Figure 3.3 The target points and normal directions.

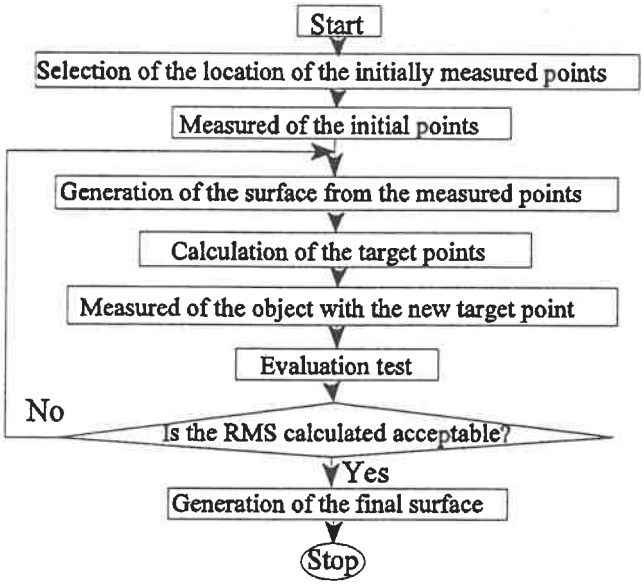

Figure 3.4 The schematic diagram for the procedure of the adaptive measurement method.

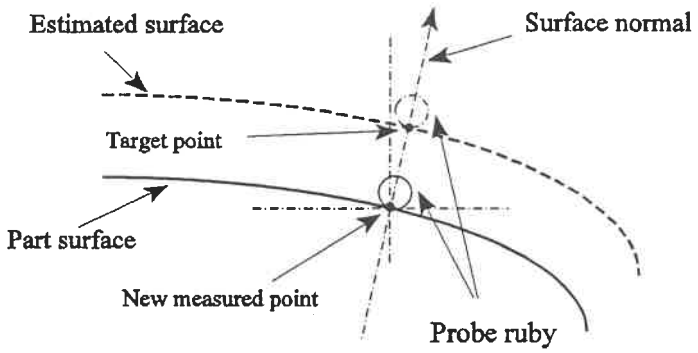

Figure 3.5 The target point and the corresponding measured point.

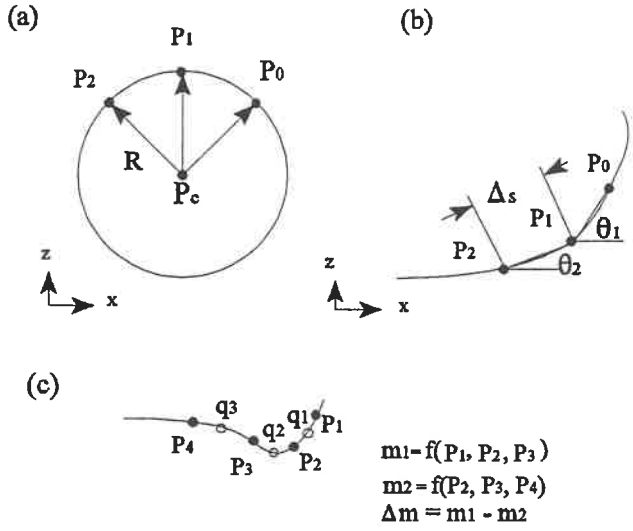

Figure 3.6 Approximating curvature: (a) osculating circle (b) ratio of tangent angle to arc length (c) the Δ m region.

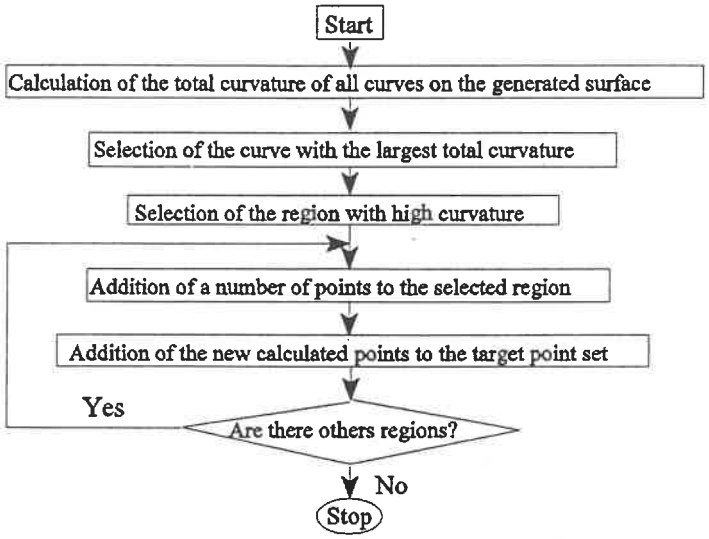

Figure 3.7 A schematic diagram for the procedure calculation of target point.

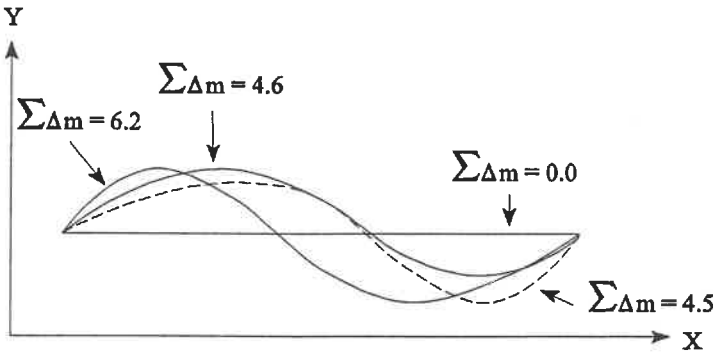

Figure 3.8 The values of Δm for differents curves.

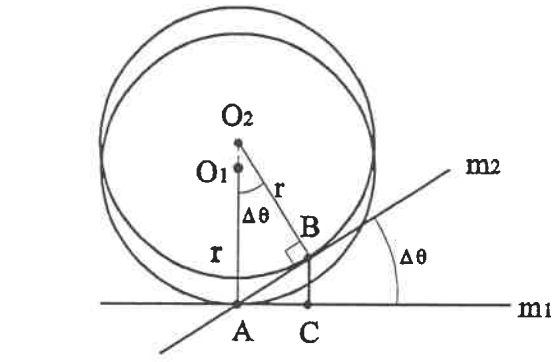

Figure 3.9 Relationship between Δm_c and $\Delta\theta_{max}$.

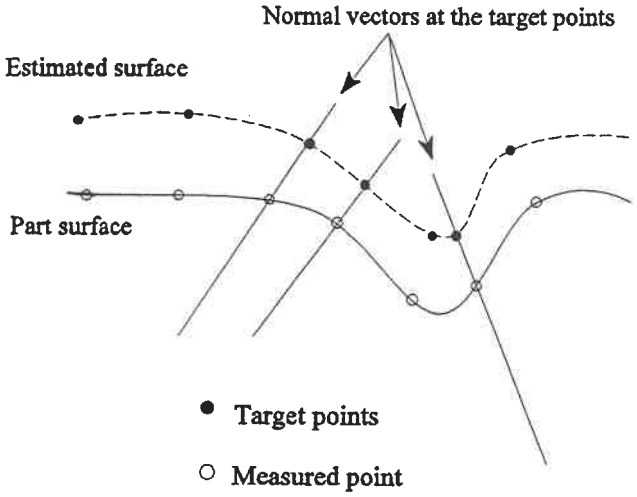

Figure 10 Relationship between the target points, normal vectors and measured points.

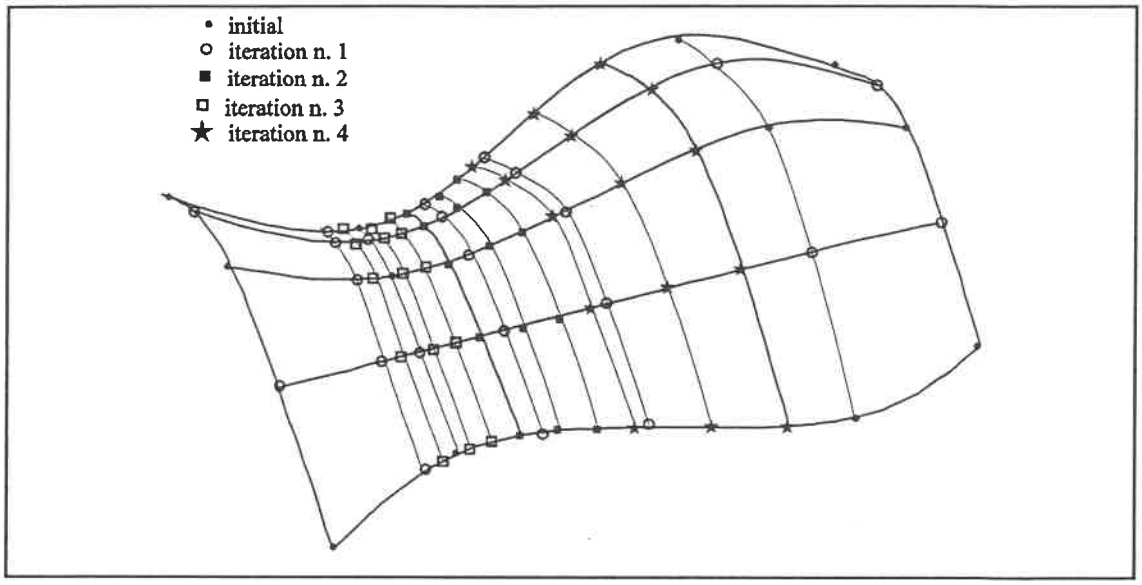

Figure 3.11 Target point locations for the initial and subsequent iteration

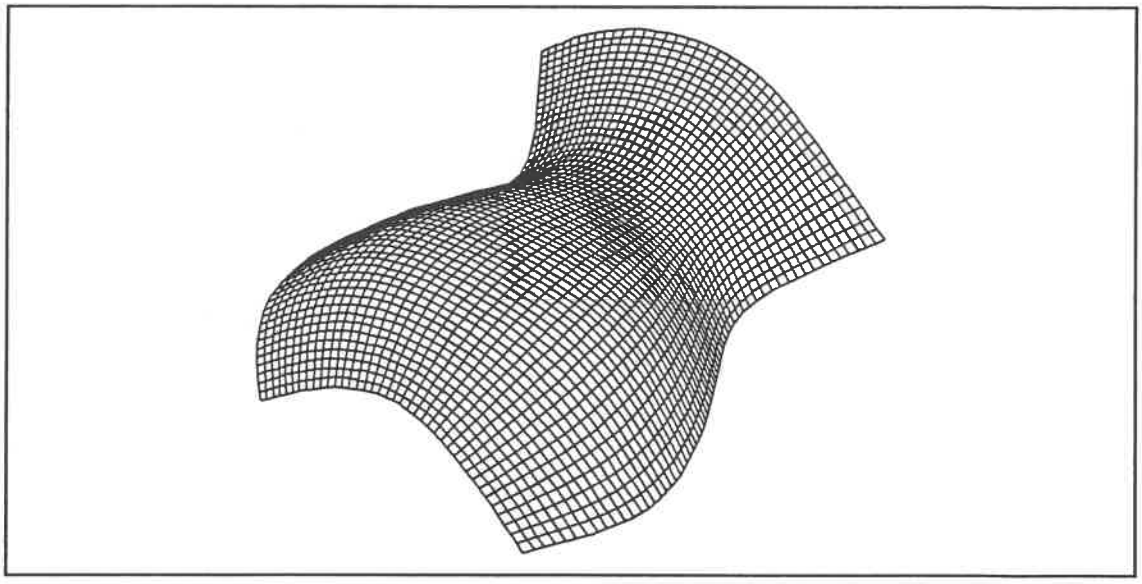

Figure 3.12 The final generated surface from the digitized part.

Chapter 4

General Conclusion and Recommendations

CONCLUSION AND RECOMMENDATIONS

In this study a CMM based methodology has been developed for reverse engineering applications. After digitizing an unknown part, the system is able to generate the surface and transfer it to a CAD system where modifications of the surface is possible. Two aspects of the problem have been addressed: 1) The compensation of the error due to the probe radius in contact with the object to be measured; 2) The automatic selection of the digitization points of an unknown surface taking a minimum number of measurements to accurately model the surface.

Both problems were solved with a model based approach using kriging to interpolate the surfaces. The probe radius compensation was performed using an approximate method by simply applying an offset to the probe centre surface. This is not theoretically correct for a general surface. However the tangential condition of touch was verified and used to validate the approximation. Since probe diameters are usually small, the approach should prove useful in most applications.

The automatic selection of measurement points represents a powerful means of not only speeding up the digitisation but also ensuring a reliable model. The surface model is progressively improved through a process of surface model estimation, verification and modification. More work is now needed to verify the optimality of the number and locations of the selected points. However the approach proved effective in precisely modelling the test part.

The ultimate aim of this research is to machine a workpiece based on measurement data on a physical model. For the digitizing step the following recommendations are made to complete this study :

1) Selection of the probe radius for different surfaces.

2) Calculation of the density of points for digitizing an object.

3) Optimisation of the inspection time using inspection planning.

4) Localization of the object for digitization and machining.

5) Harmonize the choice of datums for the workpiece, CMM inspection, CAD modelling and CNC machining.

References

[1] MacINNIS P., (1990), "The metamorphosis of phototyping", CAD/CAM System, Dec., pp. 14-17.

[2] POLHEMUS Inc. Brochure on 3SPACE Digitizer, Colchester, Vermont (1991).

[3] Science Accessories Corporation, Brochure on GP-8-3D Sonic Digitizer, Stratford, CT (1989).

[4] MOTAVALLI S. and Bidanda B., (1991) "Development of a part image reconstruction system for reverse engineering of design modifications", J. Manufacturing Sys., **10**(5).

[5] ROKER F. and KIESSLING A., (1975) "Methods for analysing three-dimensional scenes", Proc. Fourth Int. Joint Conf. Artificial Intelligence, Tabilisi, Georgin, USSR, Sept., pp. 669-673.

[6] SHIRAI Y. and SUMA M., (1971) "Recognition of polyhedrons with a range finder", Proc. Second Int. Joint Conf. Artificial Intelligence, London, pp. 80-87.

[7] SHIRAI Y., (1987) "Three dimensional Computer Vision", Springer-Verlag, London, pp. 122-140.

[8] MA W., KRUTH J.P., (1994) "Mathematical modelling of free-form curves and surfecs from discrete points with NURBS", Curves and Surface in Geometric Design, A.K. Peters, Boston.

[9] KRIGE, D. G. (1951) A statistical approach to some basic mine valuation problems on the witwatersrand. *J. Chem. Metal. Min. Soc. S. Afr.*, S2, 119-139.

[10] TROCHU, F. (1993) A contouring program based on dual kriging interpolation.

Engineering with Computers, Vol 9, 160-177.

[11] VIKERS G. W., LY M.H. and OETTER R.G., "Numerically controlled machine tools", Ellis Horwood Publishers.

[12] FAUX, I. D., PRATT, M. J. (1980) *Computational Geometry for Design and Manufacturing*, Elliss Horwood Publishers.